The Geological Society Special Publications

Sedimentary dynamics and topographic controls on the tidal-dominated Zagra Strait, early Tortonian, Betic Cordillera, Spain

--Manuscript Draft--

Manuscript Number:	GSLSpecPub2021-85R2
Article Type:	Article
Full Title:	Sedimentary dynamics and topographic controls on the tidal-dominated Zagra Strait, early Tortonian, Betic Cordillera, Spain
Short Title:	Sedimentary dynamics of the Zagra Strait
Corresponding Author:	Carlos Braga Universidad de Granada Granada, Granada SPAIN
Corresponding Author E-Mail:	jbraga@ugr.es
Other Authors:	Ángel Puga-Bernabéu
	Julio Aguirre
	José M Martín
Order of Authors (with Contributor Roles):	Juan Braga (Conceptualization: Equal; Investigation: Equal; Visualization: Equal; Writing – review & editing: Equal)
	Ángel Puga-Bernabéu (Conceptualization: Equal; Investigation: Equal; Methodology: Equal; Software: Lead; Visualization: Lead; Writing – original draft: Lead; Writing – review & editing: Lead)
	Julio Aguirre (Conceptualization: Equal; Funding acquisition: Lead; Investigation: Equal; Methodology: Equal; Writing – review & editing: Equal)
	José M Martín (Conceptualization: Equal; Investigation: Equal; Validation: Equal; Writing – review & editing: Equal)
Abstract:	The approximately 350 m-thick stratigraphic succession of the Zagra Strait records an important oceanographic phase of basin interconnection between the Atlantic Ocean (Guadalquivir Basin) and the Mediterranean Sea through the Betic Cordillera (southern Spain) during the early Tortonian. The Zagra Strait developed as a narrow structurally-controlled marine corridor. The sedimentary dynamics of the Zagra Strait was interpreted from the sedimentological features observed in six sections at well-exposed outcrops. Large-scale (>10 m high) compound and compound-dune complexes moved parallel to the strait margins under strong tidal currents generated by tidal amplification at the strait entrance and exit. Dune distribution can be divided in three sectors with different palaeocurrent migration, lithological and topographical characteristics. The northern and central sectors were separated by a deep depression (>75 m water depth) where tidal currents were weaker and dunes were not generated. The southern sector records a relative decrease in current strength compared with the northern and central sectors, and a significant increase in the bioclastic content in the sediment. Terrigenous content generally increases towards the strait margins, and reciprocally, carbonates towards its axis. The closure of the Zagra Strait resulted from tectonic uplift of that part of the Betic Cordillera before the late Tortonian.
Section/Category:	Straits and Seaways: controls, processes and implications in modern and ancient systems
Additional Information:	
Question	**Response**
Are there any conflicting interests, financial or otherwise?	No
Samples used for data or illustrations in	Confirmed

this article have been collected in a responsible manner	
Data Availability Statement	All data generated or analysed during this study are included in this published article.
Competing Interests Statement	We declare that we have no known competing financial interests or personal relationships that could have appeared to influence the work reported in this paper.

Sedimentary dynamics and topographic controls on the tidal-dominated Zagra Strait, early Tortonian, Betic Cordillera, Spain

Ángel Puga-Bernabéu[1*], Juan Carlos Braga[1], Julio Aguirre[1] and José Manuel Martín[1]

[1] *Departamento de Estratigrafía y Paleontología, Universidad de Granada, 18002, Spain*

ORCID ID: 0000-0002-6420-9167; 0000-0002-2657-0584; 0000-0002-7873-4544; 0000-0003-4742-5252

*Corresponding author (e-mail: angelpb@ugr.es)

Abstract: The approximately 350 m-thick stratigraphic succession of the Zagra Strait records an important oceanographic phase of basin interconnection between the Atlantic Ocean (Guadalquivir Basin) and the Mediterranean Sea through the Betic Cordillera (southern Spain) during the early Tortonian. The Zagra Strait developed as a narrow structurally-controlled marine corridor. The sedimentary dynamics of the Zagra Strait was interpreted from the sedimentological features observed in six sections at well-exposed outcrops. Large-scale (>10 m high) compound and compound-dune complexes moved parallel to the strait margins under strong tidal currents generated by tidal amplification at the strait entrance and exit. Dune distribution can be divided in three sectors with different palaeocurrent migration, lithological and topographical characteristics. The northern and central sectors were separated by a deep depression (>75 m water depth) where tidal currents were weaker and dunes were not generated. The southern sector records a relative decrease in current strength compared with the northern and central sectors, and a significant increase in the bioclastic content in the sediment. Terrigenous content generally increases towards the strait margins, and reciprocally, carbonates towards its axis. The closure of the Zagra Strait resulted from tectonic uplift of that part of the Betic Cordillera before the late Tortonian.

Straits and seaways are, respectively, narrow and wide marine passageways flanked by emergent land areas that connect two basins (Longhitano and Steel, 2016). Driven by the continental drift, they have played a key role in modulating global ocean circulation and influencing climate during the geological history, especially during the Cenozoic (Murdock et al., 1997; Martín et al., 2001; Livermore et al., 2007; Zhang et al., 2014; Scher et al., 2015, Capella et al., 2018). The closure of straits promoted the interchange of terrestrial fauna and division of marine organisms, driving major biotic reorganizations on land and at sea (Webb, 1976, 2006; O'Dea et al., 2016). In the Betic Cordillera (S Spain), tectonic uplift caused by the convergence between the Eurasia and African plates since the early Miocene (Sanz de Galdeano, 1990; Duggen et al., 2003; Platt et al., 2013) resulted in several episodes of narrowing of oceanographic connections that led to the formation and progressive closure of the North Betic, Zagra, Dehesas de Guadix and Guadalhorce Corridor straits (Martín et al., 2001, 2009, 2014; Betzler et al., 2006; Braga et al., 2010). The continuous uplift, restriction of the marine connections, strait emergence and eventual closure of the Betic straits during the late Miocene led, together with the closure of the

Rifian corridors to the isolation of the Mediterranean Sea that culminated at ~6 Ma with the Messinian Salinity Crisis (Hsü et al., 1973; Achalhi et al., 2016).

Many straits are defined as tidal straits because of the amplification of tidal currents due to the restriction of the cross-sectional area along them (Defant, 1961; Pugh, 1987), even in microtidal seas such as the Mediterranean Sea (Longhitano, 2018a). Tidal currents flow in reversal phases generating dunes that usually migrate outwards of the strait, although they can locally migrate in the opposite direction to the dominant current (Longhitano and Steel, 2016). Ancient tidal strait deposits are relatively unknown in the rock record, but they have been documented in the western U.S.A. (Gardner and Dorsey, 2021; O'Connell et al., 2021) and in a number of case studies within the Mediterranean Sea, being the best-known examples from the Calabrian Arc (Longhitano, 2018b; Longhitano et al., 2012, 2014), Corsica-Sardinia block (Reynaud et al., 2013; Telesca et al., 2020) and the Betic Cordillera (Martín et al., 2009, 2014). The sedimentary record of these narrow and relatively shallow-water (<150 m) straits is characterized by the presence of giant (>10 m in height) cross-stratification formed by migration of large dunes moved by strong currents amplified by the constricted morphology of the strait. Sedimentary models of ancient tidal straits are scarce, as the sedimentary dynamics in the strait is usually interpreted just from palaeocurrent analyses. However, the distribution of strait deposits and related facies (e.g., tidal deltas, carbonate factories) depends on the variations of tidal current strength along the strait and distinct depositional zones can be distinguished (Longhitano, 2013).

The sedimentary record of the straits connecting the Mediterranean Sea and the Atlantic Ocean through the Betic Cordillera during the Miocene indicates that they were either density current (outflowing from the Mediterranean)- or tidal current-dominated (Martín et al., 2014). Martín et al. (2014) interpreted the large-scale cross-strata in Miocene rocks cropping out at the transition from the northwestern margin of the Granada Basin to the Guadalquivir Basin as the result of submarine dunes migrating along a narrow corridor under the influence of tidal currents (i.e., the Zagra Strait). In this work, we contribute to the knowledge of ancient tide-dominated straits by documenting the sedimentological features of the Zagra Strait deposits and their spatial and temporal distribution, interpreting its sedimentary dynamics within the context of existing facies models. We also attempt a reconstruction of the Zagra Strait in a palaeogeographic setting dominated by regional tectonic uplift, providing age constraints to improve the palaeogeographic reconstructions of the Atlantic-Mediterranean Betic connections during the Miocene.

Geological context

The Zagra Strait is located in the Subbetic domain in the External Zones of the Betic Cordillera (Fig. 1A), the westernmost segment of the Alpine mountain belt. The External Zones comprise Mesozoic to middle Miocene age rocks that constitute the deformed sedimentary cover of the southern margin of the Iberian plate (García-Hernández et al., 1980), in contrast to the other major domain of the cordillera, the Internal Zones, mainly composed of metamorphic complexes (Fallot, 1948; Sanz de Galdeano, 1997). The Subbetic domain includes the more distal deposits within the External Zones (García-Hernández et al., 1980).

The Zagra Strait was part of the Neogene Betic basins, which consist of a number of intermontane basins and the foreland Guadalquivir Basin (Sanz de Galdeano and Vera, 1992). The intermontane basins occur both in the Internal and the External Zones. Most of them were linked to the Mediterranean Sea as marginal depocenters of the Alboran Basin, whilst a few others were embayments at the southern margin of the Guadalquivir Basin and were palaeogeographically linked to the Atlantic Ocean (Braga et al., 2002). The evolution of the Neogene basins reflects regional uplift since the late Miocene, which took place under compression due to continuous convergence of the Eurasian and African plates (Galindo-Zaldívar et al., 2019). Uplift and emersion of the mountain chain caused the progressive closure of the connections between the Atlantic Ocean and the Mediterranean Sea through the Betic Cordillera (Esteban et al., 1996; Braga et al., 2003; Martín et al., 2014). One of these gateways was the Zagra Strait, which connected the northwestern end of the Mediterranean-linked Granada Basin with the central sector of the foreland Guadalquivir Basin (Fig. 1).

The Zagra Strait deposits unconformably overlie previously folded and faulted Triassic to middle Miocene sedimentary rocks. The 12-km long and 7-5 km wide outcrop belt of strait deposits is roughly aligned in a NNW-SSE direction (Fig. 1C), parallel to a major extensional fault system consistent with the NNW–SSE to N–S compression regime of the cordillera since the Tortonian (Rodríguez-Fernández and Sanz de Galdeano, 2006; Galindo-Zaldívar et al., 2019). As consequence of the compressional context, the strait deposits were in turn overthrusted by older rocks and affected by faulting in later stages of regional evolution.

Material and methods

The strait deposits were investigated in six sections at well-exposed outcrops grouped in three sectors: northern sector (Fuentes del Cesna and El Morrón sections), central sector (Zagra, Ventorros de San José, and Las Martillas sections) and southern sector (Los Arenales section) (Fig. 1C).

This field-based study was complemented with drone photogrammetry to improve the geological analysis and constrain the depositional architectures on vertical cliffs in most of the study outcrops. The distribution of the Zagra Strait outcrops was analysed by mapping at 1:10000 scale, including the distribution of the underlying fine-grained sediments that provided an age control. Three representative stratigraphic sections, ranging from 130 to 210 m in thickness, were logged in selected outcrops to characterise the lithofacies succession (Fig. 1C). Lithofacies were defined on the basis of field descriptions, such as lithology, grain size, texture, bioclastic content and sedimentary structures, and supported by petrographic analysis of 25 thin sections. Biostratigraphic dating is based on planktonic foraminifera assemblages picked up from four washed silty marl samples.

The scanning and photograph acquisition on the study outcrops was carried out using two ready-to-fly drones helped with a GPS system Geomax Series Zenith25 PRO for the acquisition of ground control points: an octocopter Atyges FV8 Topodron carrying a Sony Nex Alpha 7 CMOS 24-megapixel camera, and a DJI Phantom 4 Pro, equipped with a DJI CMOS 20-megapixel camera. Total flight time (without including batteries change) ranged from 20 to 35 minutes at each site. Photos were taken every three seconds and/or radio-controlled with the drone stationary for specific details. The construction of the three-dimensional photogrammetric outcrop models was carried out using the software Agisoft Metashape v. 1.6.2. Between 400 and 800 photographs were processed for generating a dense point cloud. The generated virtual outcrop models were exported to the software Virtual Reality Geological Studio v. 2.64 (Burnham and Hodgetts, 2019) for geological analysis (geometry, dimensions of the sedimentary bodies and their three-dimensional spatial relationships, measurement of cross-strata orientation, etc.). The resolution of the virtual outcrop models was high enough to visualize and correctly measure cross strata of larger than 0.35 m in thickness. Grapher 13 was used to plot rose diagrams and histograms.

The cross-set thickness is described following Ashley (1990) classification as: thin (<40 cm), medium (40-75 cm), thick (75-500 cm) and very thick (>500 cm). The internal organization of the cross-stratified sets is described according to Anastas et al. (1997) as: single (cross-sets with conformable strata or laminae), compound (cross-sets with an internal discontinuity surface) and compound-compound or compound-dune complex (cross-sets with two orders of discontinuities). In each study outcrop and regardless the hierarchy of the bounding surfaces (e.g., Anastas et al., 1997; Olariu et al., 2012), the set boundaries of the cross strata defining a bedform are classified according to their size. Exceedance probability (P_{ex}) plots of bidirectional cross strata were constructed to study the dominance of the flow direction based on the percentage of given cross strata thickness to be equalled or exceeded:

$$P = \frac{m}{n+1}$$

Where m represents the rank of the cross strata thickness and n the total number of data measurements recorded.

Results

Lithofacies of the strait deposits

The stratigraphic infill of the Zagra Strait is composed of siliciclastic and mixed silici-bioclastic sediments arranged in cross-stratified beds that include single sets and cosets ranging in thickness from ~25 cm up to ~30 m. Six main lithofacies occur in the studied outcrops with varying thicknesses and slight differences in their abundance (Figs. 3 and 4):

a) Pebbly conglomerates: they are matrix supported oligomictic, rounded to subrounded conglomerates that include 1-3 cm clasts and minor cobbles up to 10 cm of quartz, chert, mudstone and marls sourced from the underlying basement rocks (Fig. 3A). This lithofacies occurs in beds from a few decimetres to a few metres thick and locally alternates with the sandstone lithofacies in thicker bedsets (Fig. 3A). Clasts in this facies can be locally subangular, giving a brechoid aspect to the bed. The matrix is similar to the sandstone lithofacies.

b) Granule to pebble conglomerates: this facies comprises granules and fine pebbles of the same nature as those in pebbly conglomerates (Fig. 3B). It can form individual beds of up to ~1.5 m in thickness to several metre-thick bedsets (Fig. 4).

c) Sandstones (Fig. 3C): this facies consists of medium- to very coarse-grained sandstones with varying degrees of cementation. Grains are mostly of rounded quartz and basement rocks. It can contain dispersed heterometric fine pebbles. Metre-scale beds of this facies commonly alternate with bioclastic gravels and mixed sandstones and gravels. This facies locally exhibits centimetre-thick bioclastic-rich bands within cross-stratified individual beds.

d) Mixed sandstones and gravels: the mixed sediment in this facies contains siliciclastic and bioclastic grains with a wide range of relative proportions, but with the siliciclastic fraction dominating over the bioclastic one (Fig. 3D). This facies forms the middle part of the continuum spectrum between the sandstones and bioclastic gravels and occurs intercalated between beds of those facies types.

e) Bioclastic gravels (Fig. 3E): this facies comprises bioclastic-dominated granule-grained to fine pebble-grained beds admixed with varying fractions of basement-derived terrigenous grains. The bioclastic components mostly include fragmented and abraded bryozoans, bivalves and coralline algae (Fig. 3E). Disarticulated complete bivalve shells can be locally preserved. Echinoids and benthic foraminifers are subordinate components. This facies builds up single cross-bedded bodies from several decimetres to several metres in thickness.

f) Bioclastic calcarenites: this facies includes medium- to coarse-grained calcarenites with a low terrigenous content (Fig. 3F). Skeletal particles are of bryozoans, bivalves, coralline algae and echinoids with minor benthic foraminifers. Its occurrence is limited to the southern part of the study area where it exhibits cross-stratified beds of varying scale.

Age constraint

In order to constrain the age of the study deposits, we analysed the planktonic foraminifer content in four marl samples (CESNA-1, FCE-11, ARENALES-W, and CJO. VIZCAINO) collected immediately underneath the strait deposits (Fig. 1C). Samples CESNA-1 and FCE-11 yielded *Globorotalia praemenardii*, *G. menardii*, *G. scitula*, *Catapsydrax unicavus*, *Paragloborotalia continuosa*, and *P. siakensis*. The first occurrence of *G. menardii* is topmost of M8 biozone and the last appearance of *G. praemenardii* took place at the top of the M9 biozone (biozonation of Wade et al., 2011). Therefore, this planktonic foraminifer assemblage can be attributed to the M9 biozone (13.34-11.71 Ma); that is, late Serravallian in age. Samples ARENALES-W and CJO. VIZCAINO include *G. menardii*, *G. scitula*, *Paragloborotalia mayeri*, *P. siakensis*, *P. continuosa*, *C. unicavus*, *C. parvulus*, and *Neogloboquadrina acostaensis*. The first occurrence of *N. acostaensis* is at the base of the Tortonian. The last appearance of *P. mayeri* and *P. siakensis* took place within the first biozone of the Tortonian; M11 (11.55-10-53 Ma) of Wade et al. (2011). This assemblage suggests a lowermost early Tortonian age, and therefore, the deposition of the Zagra Strait facies postdates the lowermost early Tortonian.

Outcrop localities

Fuentes del Cesna. This section is located west of the Fuentes del Cesna village, at the northwestern margin of the study area, the closest to the Guadalquivir Basin among described outcrops (Fig. 1B, C). Medium- to coarse-grained sandstones, sandstones with alternating bioclastic-rich bands and intercalated 1 to 1.5 m-thick conglomerate beds dominate the ~210-m thick strait succession at this locality (Fig. 4). This succession is organized in trough cross-stratified bodies that range in thickness between 8 and 18 m (very thick strata) and several hundred metres wide (Fig. 5). The basal deposits fill an irregular surface excavated in late Serravallian-lowermost early Tortonian marls and silty marls (Figs. 1C and 4), which in turn unconformably overlie the Subbetic basement. The general palaeocurrent orientation of these large-scale structures indicates a vertical change in the migration direction of the cross-stratified bodies from S to WNW-NW (Fig. 5A). The internal architecture of the cross-bedded bodies includes 1 to 5 m-thick single and compound cross-bedded foresets (Fig. 5). The reactivation surfaces are concave-up with decimetre-scale erosional relief in the thick trough cross-bedded strata (Fig. 5C). The smaller dunes and compound dunes generally migrate in the same direction as their larger parent structures. However, in some cross-bedded bodies the smaller-scale cross-beddings clearly exhibit an asymmetrical bidirectional (N-S) foreset migration (Fig. 5D). The size distribution of these cross-bedded strata is left-side skewed and there is a slightly predominant trajectory of structures >2 m towards the south (flood tidal current), which also corresponds to the larger structures (Fig. 5D).

Soft-sediment (plastic) strata deformation is common in the Fuentes del Cesna outcrop (Fig. 4). The deformation occurs as complex and simple folds. Complex folds affect to the entire thickness (several metres) of the large cross-bedded bodies (Fig. 5E). These folds show a variety of shapes and sizes, and their abundance, asymmetry (locally overturned) and complexity decreases upwards within individual bodies from the axis of the trough. Single folds affect individual strata of smaller-scale cross-bedded sets within the large cross-bedded bodies. These folds are generally symmetrical (vertical fold planes) or slightly inclined toward the dip direction of undeformed cross-beds within the same set (Fig. 5C, E). The upper part of simple folds can be locally truncated by overlying undeformed cross beds, commonly of a different and larger-scale structure. Locally, oblique sand injectites, a few centimetres wide and up to 120 cm high, intrude the cross-bedded sandstones.

El Morrón. The El Morrón section is located 1 km southeast of the Fuentes del Cesna section (Fig. 1C). Here, the Zagra Strait deposits crop out along a well-exposed cliff and unconformably overlie and onlap substrate marls. The strait succession is ~130 m thick and forms a SE-dipping tabular-strata complex made up of pebbly conglomerate, granule to pebble conglomerate and sandstone facies. The internal architecture of this complex consists of up to 8 m-thick sets of clinoforms and tabular sheets, and 0.5- to 2-m thick and a few tens of metres wide, single and compound planar and trough cross-bedded sets (Fig. 6). Clinoform foresets and sheet strata dip 18-25º consistently towards SE (115º to 130ºN). Individual beds within the tabular sheets are continuous for a few hundreds of metres in the down-current direction. Clinoforms and sheets are more abundant to the upper part of the section. Trough cross beds are a few tens metres wide and exhibit a dominant direction of foreset migration towards the southeast. Planar cross beds are located in the lower part of the section and are separated from the overlying sediments by a planar surface laterally continuous at least along 400 m (Fig. 6A, D). Planar tangential foresets extend over several tens of metres towards N (N320º to 40ºN) (Fig. 6C). Reactivation surfaces that separate the single and compound cross-bedded sets dip 6-20º southwards regardless the orientation of the cross beds.

Locally, blocks of fine-grained sandstones are engulfed within tabular sheets and cross-bedded sets. These blocks are up to 7 m wide and well rounded (Fig. 6D). Blocks were placed on top of planar cross-bedded sets and deformed the underlying cross strata. Overlying deposits adapted to the block relief. Syn-sedimentary activity is evidenced by high-angle normal faults affecting the lower part of the strait succession dominated by planar cross beds. The faults are sealed by trough cross beds, tabular sheets and clinoforms. Soft-sediment deformation of cross-strata is also locally observed in the lower part of the section. This includes buckled foresets (*sensu* Allen, 1982) that transition in the foreset dipping direction to complex folds.

*Zagra***.** The very well-exposed outcrops around the village of Zagra include a 120 m-thick succession of cross-stratified siliciclastic and lesser carbonate deposits that onlaps marls and marly limestones from the Subbetic basement. The cross-stratification deposits of this outcrop are subdivided into four scale classes based on the foreset size and relative orientation of bounding surfaces (Fig. 7A). The very large cross-stratified bodies (class 1) comprise 15 to 30 m thick cross sets bounded by major master surfaces that define troughs up to few hundreds of metres wide. The thickness of the preserved foresets increases upwards. Class 1 cross-stratified bodies include a number of 2 to 6 large, 2.8 to 18 m thick and several tens of metres wide trough cross-bedded sets (class 2). Their concave-up set bounding surfaces scour down to a few metres in the underlying cross strata. Internally, beds can locally be slightly folded towards the trough axis (Fig. 7B). Medium-scale cross-stratified bodies encompass 1 to 5 m thick and metres to tens of metres wide trough cross-bedded sets (class 3). Their bounding surfaces have overall decimetre-scale erosional relief and on the deeper scours cross beds progressively flatten up on the underlying surface. The smaller-scale cross-stratification (class 4) corresponds to 0.35 to 1.5 m thick foresets. These small-scale cross beds do not occur in all medium-scale cross strata. Palaeocurrents obtained from cross-bedded foresets and trough axes indicate a consistent migration of bedforms of varying sizes towards NE (Fig. 7A).

Ventorros de San José. The Zagra Strait deposits in this section crop out along the road that connects Ventorros de San José and Algarinejo villages (Fig. 1C). The Ventorros de San José section includes a 145 m-thick succession that is in lateral and stratigraphical continuity with the Zagra section and onlaps against Triassic clays, marls, sandstones and breccias of the basement. The lowermost part of the succession comprises alternating 1 to 3 m thick beds of varying facies types, from pebbly conglomerates to bioclastic gravels (Fig. 4). They are overlain by a ~60 m-thick interval of granule to pebble conglomerates and mixed sandstones and gravels. The upper half of the logged section consists of a lithologically monotonous succession of granule to pebble conglomerates with some intercalated conglomerate beds (Fig. 4).

The internal architecture of the strait succession includes mostly single and compound trough cross-beds and minor planar cross strata (Fig. 8). Thickness of the compound cross strata is between 2.8 and 10.9 m, and the average height of the foresets in single cross-beds is 2.5±0.4 m. Foresets are tangential or angular and within single cross-bedded bodies they can reach up to 150 m in the down-current direction (Fig. 8A, B). They exhibit a bidirectional migration pattern, from N-NE to S-SE (Fig. 8). Southward-oriented foresets are more abundant, but the size distribution of the northward- and southward-oriented cross strata are similar (Fig. 8C). Maximum foreset inclination is between 5° and

15°. The set boundaries of compound cross strata are planar and gently dipping downwards, commonly ~5° and only locally exceeds 10° (Fig. 8A, B).

Las Martillas. Well-exposed strait deposits crop out along the cliffs and steep slopes of the Las Martillas hill, 2.5 km southwest of Ventorros de San José village (Fig. 1C). The ~135-m thick succession unconformably fills and onlaps an irregular surface excavated on limestones and marls from the basement. Sandstones, mixed sandstones and bioclastic gravels alternate forming thickening- and coarsening-upwards cycles ranging from 19 to 35 m in thickness (Fig. 4). A few conglomerate and granule to pebble conglomerate beds are intercalated. These facies are organized in very thick (up to 20 m) trough cross strata (Figs. 4 and 9) with directional foreset migration towards the NW and SE (Fig. 9A, B). The larger (generally >5 m) cross-stratified bodies are internally formed by smaller-scale cross beds of at least two orders that vary between 2 m thick ripple lamination (Fig. 9C, D). These smaller-scale structures also exhibit a general bidirectional foreset migration to NW and SE (Fig. 9D), although northward-oriented structures >2 m thick slightly prevail over the opposite direction (Fig. 9D). Soft-sediment deformation is locally observed in medium-thick northward-oriented cross beds, where it occurs as buckled foresets.

Los Arenales. This section is located in the southernmost part of the study area, at the eastern side of the Genil River and 4 km northwest of Loja town (Fig. 1C). The strait deposits are well exposed along a 20 to 40 m high NE-SW-oriented cliff (Fig. 10A). The sedimentary succession is lithologically homogeneous and composed of bioclastic calcarenites. It is arranged in single and compound cross strata of varying size and orientation. Larger structures correspond to 10-12 m thick cross-bedded sets dipping to S-SW (Fig. 10A). Smaller-scale structures correspond mostly to single and compound planar cross-bedding with tangential and angular foresets up to 2.7 m high migrating either northwards or southwards (Fig. 10B, C). Northwards-oriented cross strata locally exhibit soft-sediment deformation. Slightly deformed cross laminae at the foreset top (buckled foresets) are sharply truncated by the overlying foresets (Fig. 10B).

Discussion

Depositional model and sedimentary dynamics

The early Tortonian cross strata exposed in the transition from the Granada Basin to the central Guadalquivir Basin are interpreted as the remnants of a marine corridor that connected both basins, the so-called Zagra Strait (Martín et al., 2014). The spatial outcrop distribution, the geometrical relationship between the strait deposits and the basement, and the palaeocurrent patterns acquired from the cross strata suggest that the Zagra Strait had a NW-SE-trending, symmetric, narrow funnelmorphology (Fig. 11), where fields of large dunes migrated subparallel to the strait margins under the action of tidal currents. Tidal currents entering narrow straits are funnelled into an area that is narrower than the radius of the amphidromic cell, resulting in cotidal lines approximately perpendicular to the strait axis (e.g., Messina Strait; Longhitano, 2018a). Therefore, and in contrast to tide-dominated coasts, flood and ebb currents follow directions roughly parallel to the strait margins (Reynaud and Dalrymple, 2012; Longhitano, 2018a). Sedimentary models based on ancient tidal-dominated straits are still relegated to a limited number of examples, and many of them are framed within the general symmetrical model of Longhitano (2013). This model points out the existence of four laterally adjacent depositional zones that extend symmetrically from the narrowest part of the strait, which is commonly the strait centre. The strait-centre zone is the area of highest current energy, and therefore, an area of sediment winnowing and bypassing, with only little gravel/shell lags over a hardrock substrate. The dune-bedded zone hosts tidal dunes, which exhibit an internal architecture indicative of tidal current dynamics. This zone transitions into the strait-end zone, where the tidal currents decelerate and fine-grained sediments are deposited. The strait-margin zone includes the side flanks of the seaway and is dominated by mass-flow processes. Our analysis of the sedimentary facies and sedimentary structures in the selected outcrops and their spatial distribution reflect some similarities and differences with the general model of Longhitano (2013).

The dune-bedded zone is the best represented in the Zagra Strait (similar to Longhitano (2013) model). Three-dimensional (3D) dunes (dunes characterized by sinuous crests that exhibit trough cross-bedding in their internal structure; Ashley, 1990) are the dominant bedforms in the Zagra Strait regardless their scale and stratigraphic position, as two-dimensional (2D) dunes (dunes characterized by straight crests that exhibit planar cross-bedding in their internal structure; Ashley, 1990) are subordinated. The dominance of 3D bedforms points to relatively strong currents as widely stated in the literature (Dalrymple et al., 1978; Allen, 1982; Southard and Boguchwal, 1990), although some flume experiments suggest that the transition from 2D to 3D dunes is related to transient excesses or deficiencies of sand that are passed from one bedform type to another (Venditti et al., 2005). In the Zagra Strait, the mean grain size and height of the foresets in the 2D and 3D dunes point to current velocities between 50 and 180 cm/s (Rubin and McCulloch, 1980) and most likely between 90 and 160 cm/s based on water depth estimations (see Strait palaeo-water depth section below) (Longhitano et al., 2014 based on bedform stability diagram redrawn from Southard and Boguchwal, 1990).

Palaeocurrent analysis points to deposition of tidal dunes in three sectors under the relative influence of southward-directed flood and northward-directed ebb tidal currents (Fig. 11). Additionally, although the stratigraphic correlation among the study sections is not straightforward, there is an upward stratigraphic change in the palaeocurrent pattern. In the northern sector (Fuentes del Cesna and El Morrón outcrops), dune migration was at first predominately dominated by southward-directed flood tidal currents (Figs. 5 and 11). Only the basal part of the El Morrón section records northward-directed cross strata. This southward-dominated palaeocurrent pattern changes towards the upper part of the Fuentes del Cesna section, where it becomes progressively symmetric (similar influence of flood and ebb currents), and finally, northward directed (Fig. 5A, D). In the central sector, the oldest record of the strait deposits corresponds to the large, ebb-dominated dunes at the Zagra outcrop (Fig. 7). Stratigraphically upwards, towards the Ventorros de San José section, and presumably to the Las Martillas section, the flood and ebb tidal currents seems to be equally strong (Fig. 8C). Finally, in the southern sector, foreset migration was also bidirectional, but under the dominance of the southward-directed flood tidal current. We interpret the palaeocurrent pattern observed in the three sectors as the result of the existence of a relatively deep depression between the northern and central sectors (Fig. 11). Flood tidal currents from the Atlantic were amplified due to the topographic constraint (both in width and depth) and decrease of the strait cross-section at Fuentes del Cesna area (Fig. 11), in a similar fashion to the modern and ancient Messina strait (Longhitano, 2018a, b). As a result, large-scale 3D dunes with smaller superimposed bedforms migrated to S-SE (Fig. 11). These dunes change in the direction of migration towards the area dominated by tabular sheets, clinoforms and medium-scale 3D dunes at El Morrón outcrop. We interpret this change in the depositional style as a consequence of a progressive increase in water depth, which leads to tidal current deceleration due to the enlargement of the cross-sectional strait area. Sediment reaching the El Morrón area accreted and prograded towards the depression, with small 3D dunes moved by the lower-energy tidal current at such water depth (Fig. 11). Reactivation surfaces in the northward-directed dunes at the lower part of the El Morrón section were inclined towards the trough, which is also in agreement with a southward deepening. These dunes were generated by the ebb current that might have accelerated towards this narrow strait area. The presence of fallen blocks and syn-sedimentary normal faults dipping southwards at the El Morrón section is consistent with the existence of a depression south of the northern sector.

The large-scale northward-migrating dune field in the central sector (Zagra outcrop) with compound dunes up to 30 m high points to very strong tidal ebb currents at relatively deep water (Fig. 11), which might have been also influenced by flow constriction over the irregular sea bottom. We interpret that this dune field was isolated from the northern sector by a deep-water depression (Fig. 11), and in contrast to the northern sector, dunes in the Zagra section do not transition into another type of bedforms indicative of weaker currents. This may suggest a sharp transition into the trough in this part of the strait. There is not field evidence of the infilling or deposition of strait sediments on the depression between the northern and central sector, but the change to northward ebb-generated bedforms in the upper part of the Fuentes del Cesna section is indicative of a change to a more classic model of current distribution, where the outgoing current in the entrance and exit of the strait is stronger than the opposite one (Allen, 1982; Dalrymple, 2010; Longhitano 2018a). The change to a clearly bidirectional palaeocurrent pattern from the Zagra section to the Ventorros de San José section is in agreement with the progressive infilling of the strait depocenter, the enlargement of the cross-section area of the strait at the central sector and the decrease of tidal current strength towards the strait margins (Frey and Dashtgard, 2011; Longhitano 2018a, b). Las Martillas section occupies a position similar to that of the Ventorros de San José section, although given its location towards the strait axis, dunes are larger due to higher current strength (e.g., LeBlond, 1983) (Fig. 11).

The relative narrowing of the strait at the southern sector (Los Arenales outcrop) caused the same effect of tidal current amplification on the flood current as in the northern entrance, generating the dominant southward-migrating large-scale dunes in the transition to the Granada Basin, with subordinated northward-migrating bedforms.

Peculiarities of the Zagra Strait

The main novelty of the Zagra Strait depositional model compared with the model of Longhitano (2013) is the existence of a depression separating the northern and central sectors (Fig. 11). In the Zagra Strait, the depression was located roughly in the strait centre, and therefore, it would be equivalent to the strait-centre zone of Longhitano (2013), but corresponding the latter to a sill instead. The different topography controls the differences in the sedimentary dynamics between the two models, although the depositional strait record is similar in both, i.e., there is little or negligible preserved sedimentary record in the strait centre. The sill in central-strait zone of Longhitano (2013) model is the zone of tidal maxima and matches with the narrowest part of the strait. Thus, sediment is bi-directionally bypassed outside the sill to areas where tidal current expansion and deceleration occur, which favours the deposition of the dune-bedded zone. The centre of the Zagra Strait corresponded to its deeper part and to a relatively wide cross-section area. Therefore, tidal currents over the depression are weaker than in the surrounding sills of the northern and central sector. In this regard, the sedimentary dynamics on the Zagra Strait depression is similar to the strait-end zone of Longhitano (2013), which is dominated by fine-grained sedimentation. An alternative explanation of the sedimentary dynamics over the depression could be that such area rather corresponds to the area of tidal and bottom stress maxima as in the model of Longhitano (2013), and the trough would be scoured by strong tidal currents in a similar way to the modern San Francisco Strait (Barnard et al., 2006, 2013). However, such interpretation is not supported by the palaeocurrent pattern observed in the northern and central sectors, which should be the opposite (i.e., southwards-directed in the Zagra section and fully northwards-directed in the Fuentes del Cesna and El Morrón sections) in case of an erosive trough in the strait centre. Towards the southern sector, the dominance of 2D over 3D dunes suggests weaker of tidal current strength likely due to less pronounced tidal amplification at the southern exit of the Zagra Strait compared with its northern entrance (i.e., different cross-sectional area).

Bidirectional trough cross-bedding at various scales is the dominant tidal sedimentary structure observed on the Zagra Strait deposits, which suggests the dominance of tidal currents over other processes such as waves, internal waves or sediment gravity flows. The relative strong currents necessary for the migration of dominant 3D dunes is in agreement with the broken and highly abraded bioclastic remains and the scarcity of burrowing. Bioturbation can be abundant or even pervasive in inter-dune areas or lateral fringes of the dune fields (Longhitano, 2018b), but such sub-environments have not been identified in the Zagra Strait. The prevalence of the orientation of cross strata with bed-thickness >2 m has been used as indicative of the flood vs. ebb current dominance in tide-dominated straits (Longhitano, 2018b). In the Zagra Strait, the dominance of flood or ebb current is not uniform along the strait (e.g., Fuentes del Cesna, Las Martillas, and Ventorros de San José sections), and therefore, it is rather due to the spatial variation of tidal current velocity and not to the differences in the dominance of the flood/ebb tidal flows along the entire strait system. Through straits connecting water masses of different densities, such as the Gibraltar and Messina straits (Hopkins et al., 1984; Bryden and Kinder, 1991), water stratification couples with tidal current amplification in the strait to control the sedimentary dynamics in the different strait zones. This coupling contributes, for example, to the tidal asymmetry as in the modern Messina strait (Longhitano, 2018a). The lack of evidence of significant tidal asymmetry (i.e., dominant flood or ebb tidal current) in the Zagra Strait suggests that water mass stratification between Atlantic and Mediterranean waters through the strait was non-existent or insignificant during the early Tortonian. This interpretation is comprehensive considering that at that time the Atlantic Ocean and Mediterranean Sea were connected through several wide seaways (Martín et al., 2014; Capella et al., 2018).

Sediment sources. The composition of the Zagra Strait deposits is indicative of a mixed terrigenous and biogenic sediment source. Additionally, the dominance of terrigenous and biogenic fractions varies along the strait (Figs. 4 and 11A). The nature of terrigenous sediments indicates they were sourced from the basement rocks and were introduced in the strait via fluvial and alluvial inputs. Minor supply could also come from erosion of the basement on the strait bottom. In the Zagra Strait, there is no record of deltas or fan deltas as observed in other tidal straits such as the North Betic and Siderno straits and other straits in the Calabrian Arc (Martín et al., 2009; Longhitano and Steel, 2016; Rossi et al., 2017). However, the high terrigenous content and its relatively coarse grain-size at the Ventorros de San José section located close to the strait margin points to a nearby input of terrigenous sediment. Breccia deposits at the Fuentes del Cesna section also suggest local terrigenous supply by debris flows. However, there is no evidence of mass-flow deposits sourced from the strait margins or erosional features such as canyons or gullies as occur, for example, in the Messina Strait (see Longhitano, 2018a, b and references therein).

Biogenic fraction is variable along the Zagra Strait, being more abundant to the south (i.e., Los Arenales section) and to the strait axis in the central sector (i.e., Las Martillas section) (Fig. 4). Biogenic components were derived from an in situ or nearby heterozoan factory. The development of carbonate factories adapted to high-energy conditions has been suggested in similar straits and seaways (Anastas et al., 2006; Longhitano, 2013; Telesca et al., 2020). Most likely, bioclastic particles were derived from factory areas on the carbonate platforms developed at the southern side of the strait (Fig. 11), where terrigenous input was likely reduced. It is also possible that some structural highs in the centre of the strait at times functioned as carbonate factories. Bioclastic-dominated cross strata in the Las Martillas section accumulated in a roughly cyclic pattern (Fig. 4), which may reflect periods of temporary decrease of siliciclastic input.

Strait palaeo-water depth. The scaling of subaqueous dune dimensions (mainly length and height) with potential controlling factors, such as grain size, flow strength or water depth, among others, has been tackled on the literature over more than 50 years (e.g., Yalin, 1964; van Rijn, 1984; Karim, 1999; Flemming, 2000; Bartholdy et al., 2005). Water depth (D) has been for long time considered the main control on dune height (H), and changes in water depth in the straits are the main driver of longer-term dune size changes. Such scaling relationship is roughly estimated as $H = 0.17D$ (Yalin, 1977) or as $H = 0.086D^{1.19}$ (Allen, 1984), and has been used to estimate the palaeo-water depth of ancient straits (Anastas et al., 1997; Martín et al., 2001, 2009). Although many field-based studies suggest that water depth cannot be considered as a major factor controlling the size of dunes (Flemming, 2000; Bartholdy et al., 2005; Franzetti et al., 2013), depth estimation from foreset height is still the most useful approach to estimate palaeo-water depth in the ancient record (see Bradley and Venditti, 2017). The new flow depth scaling approach presented by Bradley and Venditti (2017) suggests that $D = 6.7H$. Based on this theoretical approach, and considering an uncertainty range bound of 50% (scaling factor of 4.4-10.1), maximum palaeo-water depth in the Zagra Strait ranged between ~75-300 m according to height of the largest compound dunes (17-30 m). These depth ranges are comparable to the depth of the dune-bedded zone in the ancient (35 to >200 m) and modern (180 to 300 m) Messina strait (Longhitano, 2018a, b). A more conservative depth of ~37-85 m is estimated considering the depth scaling from the highest individual foresets (8.5 m at the Zagra section). This depth may apply to the shallower part of the Zagra Strait and is similar to the depth of the single large dunes (6-10 m high) in the San Francisco Bay strait lying at 30-106 m water depth (Rubin and McCulloch; 1980; Barnard et al., 2006). These depth estimations are also consistent with the location of the deepest part of the dune-bedded strait in the Zagra area, where the strongest tidal currents at a certain critical water depth were associated with the largest dunes, close to the interpreted depression between the northern and central sectors. Given the complex internal architecture of the large dunes formed by superimposed bedforms of varying hierarchical orders (e.g., Anastas et al., 1997), and since foreset height must be considered the minimum preserved height (Allen, 1980; Longhitano et al., 2014), a depth range of 75-300 m seems reasonable as the maximum depth for the dune-bedded zone in the Zagra Strait.

Syn-sedimentary processes. The sedimentary infilling of the Zagra Strait records soft-sediment deformation and growth fault deposits that took place syn-sedimentarily or just after sediment deposition when sediment was still unconsolidated. Soft-sediment deformation is dominant towards the northern side of the strait, especially at Fuentes del Cesna section, where large-scale 3D dunes are collapsed (slumped) (Fig. 5E) and some smaller-scale dunes are slightly deformed. The relatively fine-grained sandy sediment at Fuentes del Cesna section compared with other strait areas might have favoured the liquefaction processes at this location (Owen and Moretti, 2011). The sharp truncation of deformed cross strata by overlying undeformed cross-beddings points to a syn-sedimentary nature of foreset deformation (Bhattacharya and Saha, 2020). In absence of evidence of biological and chemical disturbances, driving forces may include differential loading, gravitational instability or shearing by tidal currents. Pounding waves during storms causing liquefaction of the dune cross strata (Okusa, 1985; Alfaro et al., 2002) seems an unlikely trigger in the Zagra Strait given the inferred depth of the bedforms. Overloading induced by sudden deposition along the lee side of the cross-strata or related to concentrated sand-laden flows along their stoss side have been interpreted in ancient tidal straits (Chiarella et al., 2016). Although we cannot discard an overloading origin for the slumped large-scale dunes, the likely origin for such disturbances in the northern side of the Zagra Strait is seismic waves triggered by earthquakes. The dimensions of the intensely deformed structures might indicate that a large amount of liquefaction was needed to affect the full strata thickness. Local sand injectites were likely originated by liquefaction triggered also by earthquakes. In contrast, cross-strata deformation in the smaller-scale dunes was most likely related to overloading processes, as the occurrence of deformation only in the upper part of the foreset laminae, including buckled foresets, are unlikely to have an allogenic origin (Chiarella et al., 20016). Deformed cross beds in the Fuentes del Cesna section occur close to the deep depression between the northern and central sectors (see section on depositional model and sedimentary dynamics). There, the deformation was likely favoured by adjacent steep slopes facing the central depression. The liquified dune mass might have subsequently moved downslope as a mass movement (Fig. 5E). The restricted occurrence of faults in specific bedsets and the presence of undeformed strata above and below agree with their syn-sedimentary origin. Also, the existence of fallen blocks engulfed between undeformed cross beds is indicative of syn-sedimentary tectonic activity. The concentration of deformations at the northern side of the Zagra Strait points to a tectonically active area that represented a relative sill lifted up along marginal faults of the central depression (Fig. 11). To the south, soft-sediment deformation is less common and its origin is not conclusive. Deformed cross strata (concentrated at the forseet top) observed in Las Martillas and Los Arenales sections most likely have an autogenic origin and can be the result of the overloading effect of concentrated sand-laden flows as interpreted in other ancient tidal straits (e.g, the Catanzaro strait; Chiarella et al., 2016), although a seismic origin related with regional tectonics as in the northern sector cannot be fully discarded. In both scenarios, deformation was a syn-sedimentary process.

Timing of the strait-fill succession and evolution of Zagra Strait

At regional scale, the Serravallian-Tortonian transition records the end of the extensional tectonics in the Betic Cordillera (García-Dueñas et al., 1992; Sanz de Galdeano and Alfaro, 2004; Rodríguez-Fernández and Sanz de Galdeano, 2006). This period was followed by a roughly N-S compressive tectonics (NNW-SSE in the study area) that extended since the Tortonian to the present (Galindo-Zaldívar et al., 1999). This change in the tectonic regime was responsible for the initial configuration of the Zagra Strait connecting the Guadalquivir Basin (Atlantic Ocean) and the Granada Basin (Mediterranean Sea) (Fig. 12A). The Zagra Strait developed as a narrow structural-controlled marine corridor related to the NNW-SSE-oriented compression and linked perpendicular extension. Relatively deep pelagic marls were uplifted in the earliest Tortonian. Subsequently, they were presumably scoured by tidal currents flowing along the new born strait as a consequence of tidal amplification, and were progressively onlapped during the strait infilling. Longhitano et al. (2014) describe a similar context for the inception of the Catanzaro Strait in the Calabrian Arc, where non-tidal fine-grained deposits are abruptly overlain by the tide-dominated strait facies. In contrast to the Catanzaro strait, the Zagra Strait succession does not record a transgressive vertical stacking where 3D dunes are replaced by 2D dunes, which in turn change progressively to small ripples and offshore mudstones (Longhitano et al., 2014). This suggests that favourable conditions for the amplification of incoming tide in the strait persisted longer in the Zagra Strait, likely associated to continued regional uplift.

The last episodes of sedimentation in the Zagra Strait are not indicative of its closure in contrast to other straits in the Betic Cordillera (Betzler et al., 2006; Martín et al., 2001, 2009). However, as in other Betic straits, the closure of the Zagra Strait resulted from the progressive tectonic uplift of the cordillera linked to the folding and thrusting of the Subbetic basement (Sanz de Galdeano and Alfaro, 2004). In absence of stratigraphic record in the strait, the timing of its closure can only be inferred from the sedimentary record in the adjacent basins previously connected through the strait. Following the Serravallian-Tortonian transition, emergent areas in the Granada Basin southeast of the Zagra Strait were progressively flooded during a transgression that lasted until the late Tortonian (Fernández and Rodríguez-Fernández, 1991; Sanz de Galdeano and Vera, 1991). The first marine unit deposited on the western margin of the Granada Basin during this transgression was a terrigenous siliciclastic unit, likely early Tortonian (Puga-Bernabéu et al., 2008). This unit comprises estuarine facies, progressively replaced by beach and platform with large sandwaves environments (Fernández and Rodríguez-Fernández, 1991). According to these authors, 'the sandwave unit' shows abundant reactivation surfaces and the palaeocurrents directions in the sandwaves are centred on easterly (N70-90E) and westerly (N280E) orientations. Fernández and Rodríguez-Fernández (1991) interpreted this unit as being deposited in a siliciclastic platform dominated by storms. These sedimentary features, however, may have a tidal origin as was identified by Martín and García-Alix (2019) in other parts of the unit.

Therefore, this terrigenous unit may reflect tidal influence from the Zagra Strait during the early Tortonian. The ongoing Tortonian transgression in the Granada Basin favoured the widespread deposition of heterozoan carbonates on shallow-water ramps (Braga et al., 1990; Fernández and Rodríguez-Fernández, 1991; Puga-Bernabéu et al., 2008; López-Quirós et al., 2016). These deposits are 9.2-7.8 Ma (Rodríguez-Fernández and Sanz de Galdeano, 2006; Puga-Bernabéu et al., 2008; Clark and Dempster, 2009; Corbí et al., 2012) and do not show evidence of any tidal signature. We argue that deposition of the carbonate unit in the Granada Basin took place after the closure of the Zagra Strait. Indirect evidence that supports this interpretation is the so-called intra-Tortonian unconformity, which resulted from an important phase of regional tectonic uplift (Vera and Gonzalez-Donoso, 1964; Estévez et al., 1982). This event was related with the Subbetic deformation and nappe emplacement and has been identified in several sectors of the Betic Cordillera, including the nearby locality of Montefrío (Gonzalez-Donoso et al., 1980; Rodríguez-Fernández, 1982; Soria, 1994; Fernández et al., 1996; Puga-Bernabéu et al., 2010; Martín-Martín et al., 2018). In the eastern Betic Cordillera, this event led to the continentalization of the marine basins, including the closure of the North Betic Strait at the end of the early Tortonian (Meijninger and Vissers, 2007; Martín et al., 2009). We argue that this tectonic event was also responsible for the closure of the Zagra Strait. We cannot state that its closure was synchronous with the closure of the North Betic Strait as the tectonic deformation linked to the subbetic thrusting belts progressed from east to west (González-Castillo et al., 2015), but it very likely occurred before the final configuration of the Granada Basin in the late Tortonian (Sanz de Galdeano and Vera, 1992; Braga et al., 2003; Rodríguez-Fernández and Sanz de Galdeano, 2006). The North Betic and Zagra straits were certainly coeval during some period during the early Tortonian. Both straits are the only ones in the Betic Cordillera that show tidal influence, which may indicate particular oceanographic and palaeotopographic conditions that favoured tidal amplification along these corridors.

After the Zagra Strait closure, marine sedimentation continued in the Granada (Mediterranean-linked) and Guadalquivir (Atlantic-linked) basins. The Granada Basin remained as a wide embayment connected with the Mediterranean Sea during the remaining Tortonian times through a relatively narrow marine seaway at its southeastern edge (Lecrín corridor) (Braga et al., 1990) (Fig. 12B). Continued regional uplift led to its progressive restriction and subsequent evaporite deposition in the latest Tortonian (7.3 to 7.2 Ma) (Martín et al., 1984; Corbí et al., 2012; García-Veigas et al., 2013) and later continentalization. In the Guadalquivir basin, heterozoan shallow-water carbonate deposition continued on thrust-top or piggyback basins developed in association with the emergent reliefs at its southern margin in the Betic Cordillera thrust and fold front (Roldán and Rodríguez-Fernández, 1991; Sanz de Galdeano and Vera, 1992).

Conclusions

The Zagra Strait developed at <10.53 Ma as a narrow marine corridor controlled by extension roughly perpendicular to the NNW-SSE-oriented compression in the Betic Cordillera. This strait connected the Mediterranean-linked Granada Basin with the Atlantic Ocean via the foreland Guadalquivir Basin during an important uplift period of the cordillera, and its deposits record the effect of tidal current amplification due to restriction of the cross-sectional area and the key role of antecedent topography in sediment distribution. Within such context and based on the sedimentological features of the Zagra Strait deposits, we found that:

(1) The Zagra strait had a morphology with two narrower sectors to the north and south and a deeper depression toward the north-central part. The strait deposits comprise a continuous spectrum from terrigenous to bioclastic carbonate sediments. Terrigenous sediments dominate towards the northern entrance of the strait and towards its margins, where particle-size is also coarser. Reciprocally, carbonate content increases towards the strait axis and its southern exit.

(2) Large-scale dunes (>10 m high) formed by superimposed, mostly 3D bedforms of up to four hierarchical orders. The dune-bedded zone was under the relative influence of southward-directed flood and northward-directed ebb tidal currents forming three sectors. In northern sector, dune migration was at first dominated by southward-directed flood tidal currents. Southward migrating dune fields built a prograding cross-strata sand body into a deep depression that separated the northern and central sectors. In the central sector, large-scale dunes moved towards the north, also stopping at the depression boundary. Increased water depth (75-300 m based on estimations from dune height) and enlargement of the cross-sectional strait area led to tidal current deceleration over the depression. A relative dominance of southward migrating large dunes occurred in the southern sector because tidal amplification at the strait exit.

(3) The preferential orientation of cross strata (i.e., flood vs. ebb current dominance) is not uniform along the strait and rather reflects spatial variation of tidal current strength instead of the dominance of the flood/ebb tidal flows in the strait system.

(4) Tectonic activity during deposition is evidenced by syn-sedimentary normal faults, sand injectites, fallen blocks engulfed between undeformed cross beds and soft-sediment deformation in the entire thickness of large-scale dunes, whose origin could also be linked to overloading processes.

(5) The closure of the strait took place as the result of the progressive tectonic uplift of the Betic Cordillera linked to the folding and thrusting of the Subbetic basement. The record of the strait closure was evidenced by the suppression of tidal influence in the nearby Granada Basin in the late Tortonian.

Acknowledgements

We thank Javier Jaimez and José Manuel Framit (Centro de Instrumentación Científica, Universidad de Granada) for their assistance with the drone flights and data processing. We thank reviewers Rebecca Dorsey, Daan Beelen and the editor Cornel Olariu for their helpful and constructive comments.

Funding

This paper has been supported by the research project PGC2018-099391-B-100 of the Spanish Ministerio de Ciencia e Innovación, and the research group RMN190 of the Junta de Andalucía.

References

Achalhi, M., Münch, P., Cornée, J-J., Azdimousa, A., Melinte-Dobrinescu, M., Quillévéré, F., Drinia, H., Fauquette, S., Jiménez-Moreno, G., Merceraud, G., Ben Moussa, A., El Kharim, Y. and Feddi, N. 2016. The late Miocene Mediterranean-Atlantic connections through the North Rifian Corridor: New insights from the Boudinar and Arbaa Taourirt basins (northeastern Rif, Morocco). *Palaeogeography, Palaeoclimatology, Palaeoecology*, **459**, 131–152.

Alfaro, P., Delgado, J., Estévez, A., Molina, J.M., Moretti, M. and Soria, J.M. 2002. Liquefaction and fluidization structures in Messinian storm deposits (Bajo Segura Basin, Betic Cordillera, southern Spain). *International Journal Earth Science*, **91**, 505–513.

Allen, J.R.L. 1980. Sand waves: a model of origin and internal structure. *Sedimentary Geology*, **26**, 281–328.

Allen, J.R.L. 1982. *Sedimentary Structures: Their Character and Physical Basis, Volume II*. Elsevier, Amsterdam, 663 p.

Allen, J.R.L. 1984. *Principles of Physical Sedimentology*. George Allen & Unwin, London, 272 p.

Anastas, A.S., Dalrymple, R.W., James, N.P. and Nelson, C.S. 1997. Cross-stratified calcarenites from New Zealand: subaqueous dunes in a cool-water, Oligo-Miocene seaway. *Sedimentology*, **44**, 869–891.

Anastas, A.S., Dalrymple, R.W., James, N.P. and Nelson, C.S. 2006. Lithofacies and dynamics of a cool-water carbonate seaway; mid-Tertiary, Te Kuiti Group, New Zealand. *Geological Society Special Publication*, **255**, 245–268.

Ashley, G. 1990. Classification of large-scale subaqueous bedforms: a new look at an old problem. *Journal of Sedimentary Petrology*, **60**, 170–172.

Barnard, P.L., Hanes, D.M., Rubin D.M. and Kvitek, R.G. 2006. Giant sand waves at the mouth of San Francisco Bay. *Eos*, **87**, 1–3.

Barnard, P.L., Schoellhamer, D.J., Jaffe, B.E. and McKee, L.J. 2013. Sediment transport in the San Francisco Bay Coastal System: An overview. *Marine Geology*, **345**, 3–17.

Bartholdy, J., Flemming, B.W., Bartholomä, A. and Emsteen, V.B. 2005. Flow and grain size control of depth-independent simple subaqueous dunes. *Journal of Geophysical Research*, **110**, F04S16, doi:10.1029/2004JF000183

Betzler, C., Braga, J.C., Martín, J.M., Sánchez-Almazo, I.M. and Lindhorst, S. 2006. Closure of a seaway: stratigraphic record and facies (Guadix basin, Southern Spain). International Journal of Earth Sciences, **95**, 903–910.

Bhattacharya, B. and Saha, A. 2020. Large soft-sediment deformation structures (SSDS) in the Permian Barren Measures Formation, Pranhita-Godavari Valley, India: potential link to syn-rift palaeoearthquake events. *Journal of Paleogeography*, **9**, 14, doi:10.1186/s42501-020-00063-z

Bradley, R.W. and Venditti, J.G. 2017. Reevaluating dune scaling relations. *Earth-Science Reviews*, **165**, 356–376.

Braga, J.C., Martín, J.M. and Alcalá, B. 1990. Coral reefs in coarse-terrigenous sedimentary environments (Upper Tortonian, Granada Basin, Southern Spain). *Sedimentary Geology*, **66**, 135–150.

Braga, J.C., Martín, J.M., Aguirre, J., 2002. Tertiary southern Spain. In: Gibbons, W. and Moreno, T. (Eds.), *The Geology of Spain*. The Geological Society, London, pp. 320–327.

Braga, J.C., Martín, J.M. and Quesada, C. 2003. Patterns and average rates of late Neogene–Recent uplift of the Betic Cordillera, SE Spain. *Geomorphology*, **50**, 3–26.

Braga, J.C., Martín, J.M., Aguirre, J., Baird, C.D., Grunnaleite, I., Bo Jensen, N., Puga-Bernabéu, A., Sælen, G. and Talbot, M.R. 2010. Middle-Miocene (Serravallian) temperate carbonates in a seaway connecting the Atlantic Ocean and the Mediterranean Sea (North Betic Strait, Spain). *Sedimentary Geology*, **225**, 19–33.

Bryden, H.L. and Kinder, T.H. 1991. Steady two-layer exchange through the Strait of Gibraltar. *Deep-Sea Research*, **38**, supplement 1, 445–463.

Burnham, B.S. and Hodgetts, D. 2019. Quantifying spatial and architectural relationships from fluvial outcrops. *Geosphere*, **15**, 236–253.

Capella, W., Barhoun, N., Flecker, R., Hilgen, F.J., Kouwenhoven, T., Matenco, L.C., Sierro, F.J., Tulbure, M.A., Yousfi, M.Z. and Krijgsman, W. 2018. Palaeogeographic evolution of the late Miocene Rifian Corridor (Morocco): Reconstructions from surface and subsurface data. *Earth-Science Reviews*, **180**, 37–59.

Chiarella, D., Moretti, M., Longhitano, S.G. and Muto, F. 2016. Deformed cross-stratified deposits in the Early Pleistocene tidally-dominated Catanzaro strait-fill succession, Calabrian Arc (Southern Italy): Triggering mechanisms and environmental significance. *Sedimentary Geology*, **344**, 277–289.

Clark, S.J.P. and Dempster, T.J. 2009. The record of tectonic denudation and erosion in an emerging orogeny: an apatite fission-track study of the Sierra Nevada, Southern Spain. *Journal of the Geological Society, London*, **166**, 87–100.

Corbí, H., Lancis, C., García-García, F., Pina, J.A., Soria, J.M., Tent-Manclús, J.E. and Viseras, C. 2012. Updating the marine biostratigraphy of the Granada Basin (central Betic Cordillera). Insight for the Late Miocene palaeogeographic evolution of the Atlantic–Mediterranean seaway. *Geobios*, **45**, 249–263.

Dalrymple, R.W. 2010. Tidal depositional systems. In: James, N.P and Dalrymple, R.W. (Eds.), *Facies Models*, **4**, Geological Association, Canada, pp. 199–208.

Dalrymple, R.W., Knight, R.J. and Lambiase, J. 1978. Bedforms and their hydraulic stability relationships in a tidal environment, Bay of Fundy, Canada. *Nature*, **275**, 100–104.

Defant, A. 1961. Water bodies and stationary current conditions at boundary surfaces. *Physical Oceanograrphy*, **1**, 451–475.

Duggen, S., Hoernie, K., van den Bogaard, P., Rupke, L. and Morgan, J.P. 2003. Deep roots of the Messinian salinity crisis. *Nature*, **422**, 602–606.

Esteban, M., Braga J.C, Martín J.M. and Santisteban C. 1996. Western Mediterranean reef complexes. In: Franseen E.K., Esteban M., Ward W.C and Rouchy J.M. (Eds), *Models for Carbonate Stratigraphy from Miocene Reef Complexes of Mediterranean Regions*. Concepts in Sedimentology and Paleontology, **5**, 55–72.

Estévez, A., Rodríguez-Fernández, J., Sanz de Galdeano, C. and Vera, J.A. 1982. Evidencia de una fase compresiva de edad Tortoniense en el sector central de las cordilleras Béticas. *Estudios Geológicos*, **38**, 55–60.

Fallot, P. 1948). Les Cordillères Bétiques. *Estudios Geológicos*, 4, 1–90.

Fernández, J., Soria, J.M. and Viseras, C. 1996. Stratigraphic architecture of the Neogene basins in the central sector of the Betic Cordillera (Spain): tectonic control and base level changes. In: Friend, P.F. and Dabrio, C.J. (Eds.), *Tertiary Basins of Spain: the Stratigraphic Record of Crustal Kinematics*. Cambridge University Press, pp. 353–365.

Fernández, J. and Rodríguez-Fernández, J. 1991. Facies evolution of nearshore marine clastic deposits during the Tortonian transgression Granada Basin, Betic Cordilleras, Spain. *Sedimentary Geology*, **71**, 5–21.

Flemming, B.W. 2000. The role of grain size, water depth and flow velocity as scaling factors controlling the size of subaqueous dunes. *In:* Trentesaux, A. and Garlan, T. (Eds.), *Marine Sandwave Dynamics: International Workshop*, 23 – 24 March 2000, University of Lille 1, France, 55–60.

Franzetti, M., Le Roy, P., Delacourt, C., Garlan, T., Cancouët, R., Sukhovich, A. and Deschamps, A. 2013. Giant dune morphologies and dynamics in a deep continental shelf environment: example of the banc du four (Western Brittany, France). *Marine Geology*, **346**, 17–30.

Frey, S.E. and Dashtgard, S.E. 2011. Sedimentology, ichnology and hydrodynamics of strait-margin, sand and gravel beaches and shorefaces: Juan de Fuca Strait, British Columbia, Canada. *Sedimentology*, **58**, 1326–1346.

Galindo-Zaldívar, J., Jabaloy, A., Serrano, I., Morales, J., González-Lodeiro, F., and Torcal, F. 1999. Recent and present-day stresses in the Granada Basin (Betic Cordilleras) 'Example of a late Miocene-present-day extensional basin in a convergent plate boundary. *Tectonics*, **18**, 686–702.

Galindo-Zaldívar, J., Braga, J.C., Martín, J.M., Aguirre, J., Puga-Bernabéu, Á., García-Alix, Marín-Lechado, C., Pedrera, A., Ruíz-Constán, A., Sanz de Galdeano, C., Ercilla, G., Casas, D., Estrada, F., Juan, C., Vázquez, J.T., and Alonso, B. 2019. Extension in the Western Mediterranean. In: Quesada, C and Oliveira J. T. (Eds.), *The Geology of Iberia: A Geodynamic Approach.* Regional Geology Reviews, Volume 4: Cenozoic Basins, Springer Nature Switzerland, pp. 61–103.

García-Dueñas, V., Balanyá, J.C., Martínez-Martínez, J.M. 1992. Miocene extensional detachments in the outcropping basement of the northern Alboran basin (Betics) and their implications. *Geo-Marine Letters*, **12**, 88–95.

García-Hernández, M., L�pez-Garrido, A.C., Rivas, P., Sanz de Galdeano, C. and Vera, J.A., 1980. Mesozoic paleogeographic evolution of the External Zones of the Betic Cordillera. *Geologie en Mijnbouw*, **59**, 155–168.

García-Veigas, J., Cendón, D.I., Rosell, L., Ortí, F., Torres Ruiz, J., Martín, J.M. and Sanz, E. 2013. Salt deposition and brine evolution in the Granada Basin (Late Tortonian, SE Spain). *Palaeogeography Palaeoclimatology Palaeoecology*, 369, 452–465.

Gardner, K. and Dorsey, R.J., 2021. Mixed carbonate-siliciclastic sedimentation at the margin of a late Miocene tidal strait, lower Colorado River Valley, south-western USA. *Sedimentology*, **68**, 1893–1922.

González-Donoso, J.M., Rodríguez-Fernández, J., Serrano, F. and Vera, J.A. 1980. Precisiones estratigráficas sobre la discordancia intratortoniense de Montefrío (Granada). *Boletín de la Real Sociedad Española de Historia Natural*, **78**, 101–111.

González-Castillo, L. Galindo-Zaldívar, J., Lacy, M.C., Borque, M.J., Martínez-Moreno, F.J. and García-Armenteros, J.A. 2015. Active rollback in the Gibraltar Arc: Evidences from CGPS data in the western Betic Cordillera. *Tectonophysics*, **663**, 310–321.

Hopkins, T.M., Salusti, E. and Settimi, D. 1984. Tidal forcing of the water mass interface in the Strait of Messina. *Journal of Geophysical Research*, **89**, 2013–2024.

Hsü, K.J., Ryan, W.B.F. and Cita, M.B. 1973. Late Miocene desiccation of the Mediterranean. *Nature*, **242**, 240–244.

Karim, F. 1999. Bed-form geometry in sand-bed flows. *Journal of Hydraulic Engineering*, **125 (12)**, 1253–1261.

LeBlond, P.H. 1983. The Strait of Georgia: functional anatomy of a coastal sea. *Canadian Journal of Fisheries and Aquatic Sciences*, **40**, 1033–1063.

Livermore, R., Hillenbrand, C.-D. and Meredith, M. 2007. Drake Passage and Cenozoic climate: An open and *shut case? Geochemistry, Geophysics, Geosystems*, **8**, Q01005. doi:10.1029/2005GC001224

Longhitano, S.G. 2013. A facies-based depositional model for ancient and modern, tectonically-confined tidal straits. *Terra Nova*, **25**, 446–452.

Longhitano, S.G. 2018a. Between Scylla and Charybdis (part 1): the sedimentary dynamics of the modern Messina Strait (central Mediterranean) as analogue to interpret the past. *Earth-Science Reviews*, **185**, 259–287.

Longhitano, S.G. 2018b. Between Scylla and Charybdis (part 2): the sedimentary dynamics of the ancient, Early Pleistocene Messina Strait (central Mediterranean) based on its modern analogue. *Earth-Science Reviews*, **179**, 248–286.

Longhitano, S.G., Chiarella, D., Di Stefano, A., Messina, C., Sabato, L. and Tropeano, M. 2012. Tidal signatures in Neogene to Quaternary mixed deposits of southern Italy straits and bays. *Sedimentary Geology*, **279**, 74–96.

Longhitano, S.G., Chiarella, D. and Muto, F. 2014. Three-dimensional to two-dimensional cross-strata transition in the lower Pleistocene Catanzaro tidal strait transgressive succession (southern Italy). *Sedimentology*, **61**, 2136–2171.

Longhitano, S.G. and Steel, R.J. 2016. Deflection of the progradational axis and asymmetry in tidal seaway and strait deltas: insights from two outcrop case studies. In: Hampson, G.J., Reynolds, A.D., Kostic, B. and Wells, M.R. (Eds.), *Paralic Reservoir: Recent Advances. Geological Society, London, Special Publications*, **444**, 141–172.

López-Quirós, A., Barbier, M., Martín, J.M., Puga-Bernabéu, Á. and Guichet, X. 2016. Diagenetic evolution of Tortonian temperate carbonates close to evaporites in the Granada Basin (SE Spain). *Sedimentary Geology*, **335**, 180–196.

Martín, J.M. and García-Alix, A. 2019. From a marine embayment to a desiccated basin: the marine to continental transition in the Granada basin (Late Miocene, SE Spain). *In: Continental-marine Interactions During the Neogene in the Mediterranean Area, Granada*, RCMNS Interim Colloquium 2019, 9-12 September 2019, Granada, Spain, Field guide, [http://hdl.handle.net/10481/56344]

Martín, J.M., Ortega-Huertas, M. and Torres-Ruiz, J. 1984. Genesis and evolution of strontium deposits of the Granada Basin (southeastern Spain): evidence of diagenetic replacement of a stromatolite belt. *Sedimentary Geology*, **39**, 281–298.

Martín, J.M., Braga, J.C. and Betzler, C. 2001.The Messinian Guadalhorce corridor: the last northern, Atlantic-Mediterranean gateway. *Terra Nova*, **13**, 418–424.

Martín, J.M., Braga, J.C., Aguirre, J. and Puga-Bernabéu, Á. 2009. History and evolution of the North-Betic Strait (Prebetic Zone, Betic Cordillera): a narrow, early Tortonian, tidal-dominated, Atlantic–Mediterranean marine passage. *Sedimentary Geology*, **216**, 80–90.

Martín, J.M., Puga-Bernabéu, Á., Aguirre, J. and Braga, J.C. 2014. Miocene Atlantic-Mediterranean seaways in the Betic Cordillera (southern Spain). *Revista de la Sociedad Geológica de España*, **27**, 175–186.

Martín-Martín, M., Guerrera, F., Rodríguez-Estrella, T., Serrano, F., Alcalá, F.J., Raffaelli, G. and Tramontana, M. 2018. Miocene tectono-sedimentary evolution of the eastern external Betic Cordillera (Spain), *Geodinamica Acta*, **30**, 265–286.

Meijninger, B.M.L. and Vissers, R.L.M. 2007. Thrust-related extension in the Prebetic (southern Spain) and closure of the North Betic Strait. *Revista de la Sociedad Geológica de España*, **20**, 153–171.

Murdock, T.Q., Weaver, A.J. and Fanning A.F. 1997. Paleoclimatic response of the closing of the Isthmus of Panama in a coupled ocean-atmosphere model. *Geophysical Research Letters*, **24**, 253–256.

O'Connell, B., Dorsey, R.J., Hasiotis, S.T. and Hood, A.V., 2021, Mixed carbonate-siliciclastic tidal sedimentation in the Miocene to Pliocene Bouse Formation, palaeo-Gulf of California. *Sedimentology*, **68**, 1028–1068.

O'Dea, A., Lessios, H.A., Coates, A.G., Eytan, R.I., Restrepo-Moreno, S.A., Cione, A.L., Collins, L.S., De Queiroz, A., Farris, D.W., Norris, R.D., Stallard, R.F., Woodburne, M.O., Aguilera, O., Aubry, M-P., Berggren, W.A., Budd, A.F., Cozzuol, M.A., Coppard, S.E., Duque-Caro, H., Finnegan, S., Gasparini, G.M., Grossman, E.L., Johnson, K.G., Keigwin, L.D., Knowlton, N., Leigh, E.G., Leonard-Pingel, J.S., Marko, P.B., Pyenson, N.D., Rachello-Dolmen, P.G., Soibelzon, E., Soibelzon, L., Todd, J.A., Vermij, G.J. and Jackson, J.B.C. 2016. Formation of the Isthmus of Panama. *Science Advances*, **2**, e1600883.

Okusa, S. 1985. Wave-induced stresses in unsaturated submarine sediments. *Geotechnique*, **35**, 517–532.

Olariu, C., Steel, R.J., Dalrymple, R.W. and Gingras, M.K. 2012. Tidal dunes versus tidal bars: The sedimentological and architectural characteristics of compound dunes in a tidal seaway, the lower Baronia Sandstone (Lower Eocene), Ager Basin, Spain. *Sedimentary Geology*, **279**, 134–155.

Owen, G. and Moretti, M. 2011. Identifying triggers for liquefaction induced soft-sediment deformation in sands. *Sedimentary Geology*, **235**, 141–147.

Platt, J.P., Behr, W.M., Johanesen, K. and Williams, J.R. 2013. The Betic-Rif Arc and its orogenic hinterland: A review. *Annual Review of Earth and Planetary Sciences*, **41**, 313–357.

Puga-Bernabéu, Á., Martín, J.M. and Braga, J.C. 2008. Sedimentary processes in a submarine canyon excavated into a temperate-carbonate ramp (Granada Basin, southern Spain). *Sedimentology*, **55**, 1449–1466.

Puga-Bernabéu Á., Martín, J.M., Braga, J.C., Sánchez-Almazo, I.M., 2010. Downslope-migrating sandwaves and platform-margin clinoforms in a current dominated distally steepened temperate-carbonate ramp. (Guadix Basin, Southern Spain). *Sedimentology*, **57**, 293–311.

Pugh, D.T. 1987. *Tides, Surges and Mean Sea-Level*. John Wiley and Sons, Chichester, 472 p.

Reynaud, J.-Y. and Dalrymple, R.W. 2012. Shallow-marine tidal deposits. In: Davis Jr, R.A. and Dalrymple, D.W. (Eds.), *Principles of Tidal Sedimentology*. Springer, New York, pp. 335–369.

Reynaud, J.-Y., Ferrandini, M., Ferrandini, J., Santiago, M., Thinon, I., Andre, J.-P., Barthet, Y., Guennoc, P. and Tessier, B. 2013. From non-tidal shelf to tide-dominated strait: the Miocene Bonifacio Basin, Southern Corsica. *Sedimentology*, **60**, 599–623.

Rodríguez-Fernández, J. 1982. *El Mioceno del Sector Central de las Cordilleras Béticas*. Ph.D. Thesis, Universidad de Granada, Spain, 224 pp.

Rodríguez-Fernández, J. and Sanz de Galdeano C. 2006. Late orogenic intramontane basin development: the Granada basin, Betics (southern Spain). *Basin Research*, **18**, 85–102.

Roldán, F.J. and Rodríguez-Fernández, J. 1991. Un ejemplo de cuenca de piggy-back asociada a la evolución neógena del frente de las Zonas Externas Béticas. Comunicaciones. In: *I Congreso del Grupo Español del Terciario*. Vic (Barcelona), 297-300 p.

Rossi, V.M., Longhitano, S.G., Mellere, D., Dalrymple, R.W., Steel, R.J., Chiarella, D. and Olariu, C. 2017. Interplay of tidal and fluvial processes in an early Pleistocene, delta-fed, strait margin (Calabria, Southern Italy). *Marine and Petroleum Geology*, **87**, 14–30.

Rubin, D. and McCulloch, D.S. 1980. Single and superposed bedforms: a synthesis of San Francisco Bay and flume observations. *Sedimentary Geology*, **26**, 207–231.

Sanz de Galdeano, C. 1990. Geologic evolution of the Betic Cordilleras in the western Mediterranean, Miocene to the present. *Tectonophysics*, **172**, 107–119.

Sanz de Galdeano, C. 1997. *La zona interna bético-rifeña: (antecedentes, unidades tectónicas, correlaciones y bosquejo de reconstrucción paleogeográfica)*. Colección monográfica. Tierras del Sur 18, 316 pp, Universidad de Granada.

Sanz de Galdeano C. and Vera J.A. 1991. Una propuesta de clasificación de las cuencas neógenas béticas. *Acta Geológica Hispánica*, **26**, 205–227.

Sanz de Galdeano C. and Vera J.A. 1992. Stratigraphic record and palaeogeographical context of the Neogene basins in the Betic Cordillera, Spain. *Basin Research*, **4**, 21–36.

Sanz de Galdeano, C. and Alfaro, P. 2004. Tectonic significance of the present relief of the Betic Cordillera. *Geomorphology*, **63**, 175–190.

Scher, H.D., Whittaker, J., William, S., Latimer, J., Kordesch, W. and Delaney, M. 2015. Onset of Antarctic circumpolar current 30 million years ago as Tasmanian Gateway aligned with westerlies. *Nature*, **523**, 580–583.

Soria, J.M. 1994. Sedimentación y tectónica durante el Mioceno en la región de Sierra Arana-Mencal y su relación con la evolución geodinámica de la Cordillera Bética. *Revista de la Sociedad Geológica de España*, **7**, 199–213.

Southard, J.B. and Boguchwal, L.A. 1990. Bed configurations in steady unidirectional water flow part 2. Synthesis of flume data. *Journal of Sedimentary Petrology,* **60**, 658–679.

Telesca, D., Longhitano, S.G., Pistis, M., Pascucci, V., Tropeano, M. and Sabato, L. 2020. Sedimentology of a transgressive middle-upper Miocene succession filling a tectonically confined, current dominated seaway (the Logudoro Basin, northern Sardinia, Italy). *Sedimentary Geology*, **400**, 105626, doi:10.1016/j.sedgeo.2020.105626

van Rijn, L.C. 1984. Sediment transport III: bedforms and alluvial roughness. *Journal of Hydraulic Engineering*, **110**, 1733–1754.

Venditti, J.G., Church, M. and Bennett, S.J. 2005. On the transition between 2D and 3D dunes. *Sedimentology*, **52**, 1343–1359.

Vera, J.A. and González-Donoso, J.M. 1964. Discordancia intravindobonense en Montefrío (Zona Subbética). *Notas y Comunicaciones del IGME*, **76**, 19–32.

Wade, B.S., Pearson, P.N., Berggren, W.A. and Pälike, H. 2011. Review and revision of Cenozoic tropical planktonic foraminiferal biostratigraphy and calibration to the geomagnetic polarity and astronomical time scale. *Earth-Science Reviews*, **104**, 111–142.

Webb, S.D. 1976. Mammalian faunal dynamics of the Great American Interchange. *Paleobiology*, **2**, 220–234.

Webb, S.D. 2006. The great american biotic interchange: Patterns and processes. *Annals of the Missouri Botanical Garden*, **93**, 245–257.

Yalin, M.S. 1964. Geometrical properties of sand waves. Journal of the Hydraulics Division, **90**, 105–119.

Yalin, M.S. 1977. *Mechanics of Sediment Transport*. Pergamon Press, 298 pp.

Zhang, Z., Ramstein, G., Schuster, M., Li, C., Contoux, C. and Yan. Q. 2014. Aridification of the Sahara Desert caused by Tethys Sea shrinkage during the Late Miocene. *Nature*, **513**, 401–404.

Figure captions

Figure 1. A) Geographical and geological schematic map of the Betic Cordillera in south Spain. GR: Guadalquivir River. Numbers mark the location of the Betic straits, from older to younger. 1: North Betic Strait; 2: Zagra Strait; 3: Dehesas de Guadix Strait; 4: Guadalhorce Strait. Modified from Martín et al. (2014). B) Location of the study area in the transition from the northwestern margin of the Mediterranean-linked Granada Basin to the central sector of the Atlantic-linked foreland Guadalquivir Basin. C) Simplified geological orthophoto-map of the study area showing the distribution of the Zagra Strait deposits and marls underneath, which unconformably overlie the Subbetic basement. Numbers

correspond to the study sections. Palaeocurrent orientation of the strait deposits are shown for each section. Asterisks mark the location of the marl samples used for biostratigraphic analysis.

Figure 2. Sketches showing the internal architecture and classification of the cross strata defining a bedform according to their size. A) Section parallel to flow direction of unidirectional very large dunes. B) Section perpendicular to flow direction of unidirectional very large dunes. C) Section parallel to flow direction of bidirectional very large dunes. Note that reactivation surfaces can occur in dunes of different sizes (e.g., a large dune can be either simple or compound).

Figure 3. Representative examples of the six major lithofacies of the Zagra Strait deposits. See figure 1c for location of the sections. A) Pebbly conglomerate bed intercalated between sandstone facies. Fuentes del Cesna section. B) Close-up view of micronglomerate facies. Note the abundance of green and red clasts derived from the terrigenous Triassic basement. Coin is 2.3 cm in diameter. Ventorros de San José section. C) Medium-thick cross-bedded sandstone facies. Hammer is 33 cm in length. D) Close-up view of the mixed sandstone and gravel facies, which represents the middle part of the continuum spectrum between the sandstones and bioclastic gravel facies. Ventorros de San José section. Coin is 2.2 cm in diameter. E) Thin to medium-thick cross-bedding in bioclastic gravels and close-up view showing the bioclastic components in this facies. Las Martillas section. F) Close-up view of a cross-laminated bed of bioclastic calcarenites. Los Arenales section.

Figure 4. Stratigraphic columns logged at three representative sections of the Zagra Strait unit (see Fig. 1C for location). f-m: fine to medium sand; m: medium sand; mc: medium to coarse sand; c: coarse sand; vc: very coarse sand; gp: granule-pebble; co: cobble. Numbers of the sections as shown in figure 1.

Figure 5. A) Northward-oriented virtual outcrop model of the eastern part of the Fuentes del Cesna outcrop showing very large trough cross-stratified bodies (major set bounding surfaces in blue). Thickness and mean migration direction are given for each of them. There is a bidirectional migration of the cross-stratified bodies, but note the upward change in the migration direction from S to N. B) Outcrop view of the contact between two very large trough cross-stratified bodies with opposite migration direction. The lower cross-stratified body includes smaller-scale, thick trough and planar cross strata. Note reactivation surfaces on the upper cross-stratified body. C) Outcrop view of the sharp erosive contact between two northward-oriented very large trough cross-stratified bodies. The upper body shows reactivation surfaces of two different orders. Slightly deformed cross beds are also marked. D) Palaeocurrent diagram and size distribution and exceedance plots of the smaller-scale cross strata that build the large trough cross-stratified body marked with an asterisk in A). Note the bidirectional pattern of the foreset migration (from trough axis and planar foresets). Orientation of isolated bedding planes of dune limbs are also shown. Foreset height distribution is slightly left-side skewed and there is a slightly prevalence of >2m-thick cross strata including S-dipping foresets over thinner N-oriented beds. E) Close-up outcrop view of an intensely deformed very large trough cross-stratified body

Figure 6. A) Eastward-oriented virtual outcrop model of the El Morrón section. Here, the Zagra Strait deposits form a large-scale tabular body that internally comprises clinoforms and tabular sheets, and planar and trough cross strata of varying scale. Asterisk mark a laterally continuous surface that

separates the lower part dominated by planar cross beds. B) Close-up outcrop view of clinoform sets. C) Outcrop view of the lower part of the El Morrón section where N-oriented cross strata dominate. Note that reactivation surfaces dip southwards. Syn-sedimentary normal faults also occur in the lower part. D) Outcrop view of a large block engulfed between cross strata. Observe that beds are deformed underneath the block and overlying cross beds adapt to its relief. This block is located on top of the area dominated by N-oriented cross-bedding. Asterisk marks the same surface than in A).

Figure 7. A) Northeast-oriented virtual outcrop model of the Zagra section showing large-scale trough cross-bedding with an internal architecture that comprises four size classes, which are marked by set boundaries of different colours. Histogram shows the relative frequency of the dune height in each size class. Foreset dips indicate a persistent migration direction towards N-NE. B) Close-up outcrop view of slightly folded cross strata towards the trough axis.

Figure 8. A) Eastward-oriented virtual outcrop model of the Ventorros de San José section showing bidirectional large-scale cross strata (shadowed areas). Palaeocurrent diagram corresponds to cross strata of varying scales. Colour code for the shadowed areas is the same as in the rose diagram. B) Close-up view showing the distinctive bidirectional pattern of the cross-bedded strait deposits at this location. Single and compound cross strata are also marked. C) Size distribution and exceedance plots of the N- and S-oriented cross strata in this outcrop. Note that the exceedance probability for cross-bedding thickness indicates that there is no prevalence of N-dipping over S-dipping foresets or viceversa, suggesting that there was no dominance of the flood or ebb tidal current at this location.

Figure 9. Northeast-oriented (A) and northwest-oriented (B) virtual outcrop model of the Las Martillas section showing large-scale bidirectional cross strata (set bounding surfaces in blue). Rose diagram based on palaeocurrent direction from cross-strata of varying size. Arrows mark the migration direction of the large cross beds. Colour code for arrows as in the rose diagram. C) Outcrop view showing the internal architecture of a large-scale trough cross-bedset consisting of smaller-scale cross strata. D) Size distribution and exceedance plots of the N- and S-oriented cross strata in this outcrop. Note the slightly prevalence of >2m-thick cross strata including N-dipping foresets over thinner S-oriented beds.

Figure 10. A) Panoramic view showing large-scale cross strata of the Zagra Strait deposits at the Los Arenales section. B) Outcrop view of smaller-scale northward-dominated cross strata consisting of single and compound dunes with tangential and planar foresets. Some cross laminae are slightly deformed in their upper part (buckled foresets) and sharply truncated by the overlying cross strata. C) Outcrop view showing bidirectional foreset migration.

Figure 11. A) Sketch illustrating the reconstruction of the Zagra Strait during the early Tortonian based on preserved outcrops. Western boundary was likely controlled by tectonics as it has the same orientation than the NNW–SSE regional faults in the area A dune-bedded strait zone is the best represented in the strait. Large-scale dunes moved roughly parallel to the strait margins under the relative influence of flood and ebb tidal currents in each sector. The widening of the strait southward of its northern entrance, and the existence of a deep depression between the northern and central sectors caused a decrease in the current strength and lack of large bedforms on the depression. The carbonate

factory at the southern margin supplied the bioclastic particles that mixed with varying proportions of terrigenous clasts in the strait sediments. Letters indicate the location of cross sections shown in B). Numbers correspond to the study sections; 1: Fuentes del Cesna; 2: El Morrón; 3: Zagra; 4: Ventorros de San José; 5: Las Martillas; 6: Los Arenales. Palaeocurrent diagrams in each section as in figures 5 to 10. B) Conceptual cross sections (see A) for location) showing the distribution of the large-scale dunes in the different strait sectors. The antecedant paleao-topography exerted an important control on sedimentary dynamics. Note the absence of bedforms on the depression between the northern and southern sectors and the clinoform and tabular sheets prograding towards the depression at the northern sector. Bioclastic carbonate content increases towards de strait axis and decreases towards the margins. A maximum depth range is estimated based on the height of the dune foresets (see text). FdD: Fuentes del Cesna Section; VSJ: Ventorros de San José section.

Figure 12. A) Early Tortonian paleogeography of the Betic Cordillera after the closure of the North-Betic Strait, showing the location of the Zagra and Dehesas de Guadix Straits. M: Málaga, G: Granada, A: Almería, J: Jaén, Mu: Murcia, Al: Alicante. B) After the closure of the Zagra Strait the Granada Basin remained open to the Mediterranean Sea. The position of the Tortonian palaeoshoreline at the active, southern margin of the foreland Guadalquivir Basin is highly uncertain due later deformation and erosion.

Figure 1

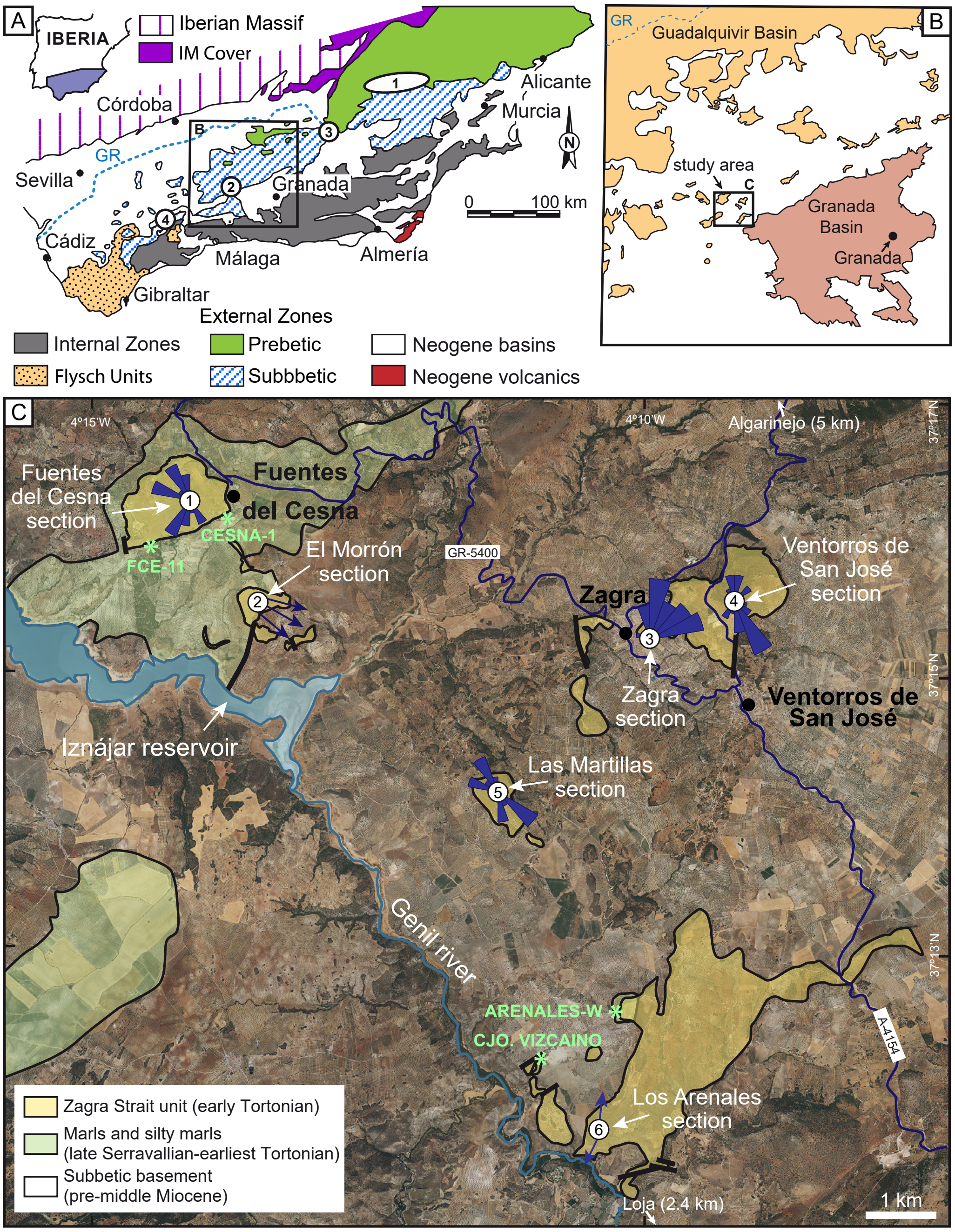
A
IBERIA
Iberian Massif
IM Cover
Córdoba
Sevilla
GR
Cádiz
Gibraltar
Málaga
Granada
Almería
Murcia
Alicante
0 100 km
External Zones
Internal Zones
Prebetic
Neogene basins
Flysch Units
Subbbetic
Neogene volcanics
B
GR
Guadalquivir Basin
study area
Granada Basin
Granada
C
4°15'W
4°10'W
Algarinejo (5 km)
37°17'N
37°15'N
37°13'N
Fuentes del Cesna section
Fuentes del Cesna
CESNA-1
FCE-11
El Morrón section
GR-5400
Zagra
Ventorros de San José section
Zagra section
Ventorros de San José
Iznájar reservoir
Las Martillas section
Genil river
ARENALES-W
CJO. VIZCAINO
A-4154
Los Arenales section
Loja (2.4 km)
1 km
Zagra Strait unit (early Tortonian)
Marls and silty marls (late Serravallian-earliest Tortonian)
Subbetic basement (pre-middle Miocene)

Figure 2

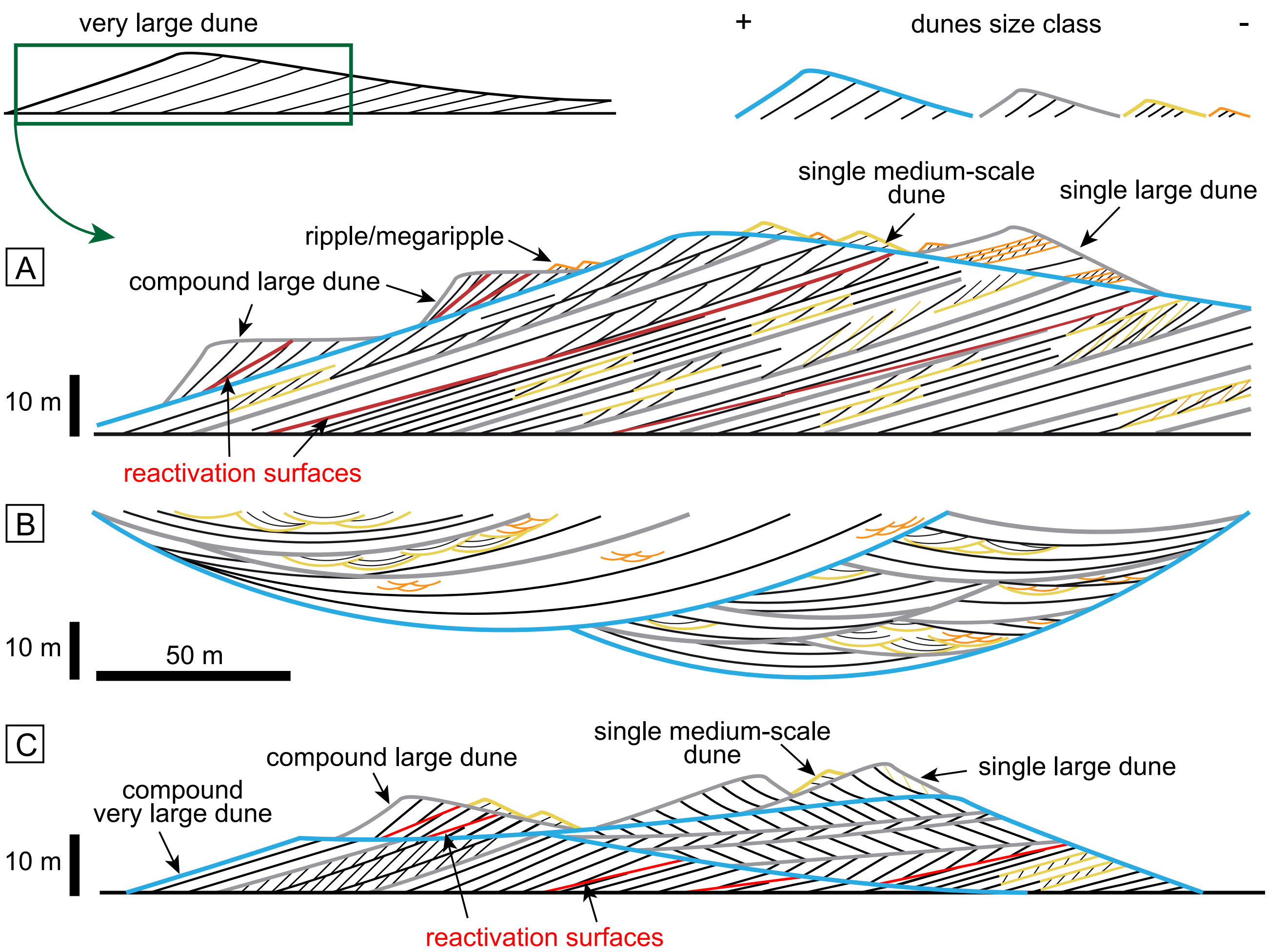

very large dune
+
dunes size class
-
A
single medium-scale dune
single large dune
ripple/megaripple
compound large dune
10 m
reactivation surfaces
B
10 m
50 m
C
single medium-scale dune
compound large dune
single large dune
compound very large dune
10 m
reactivation surfaces

Figure 3

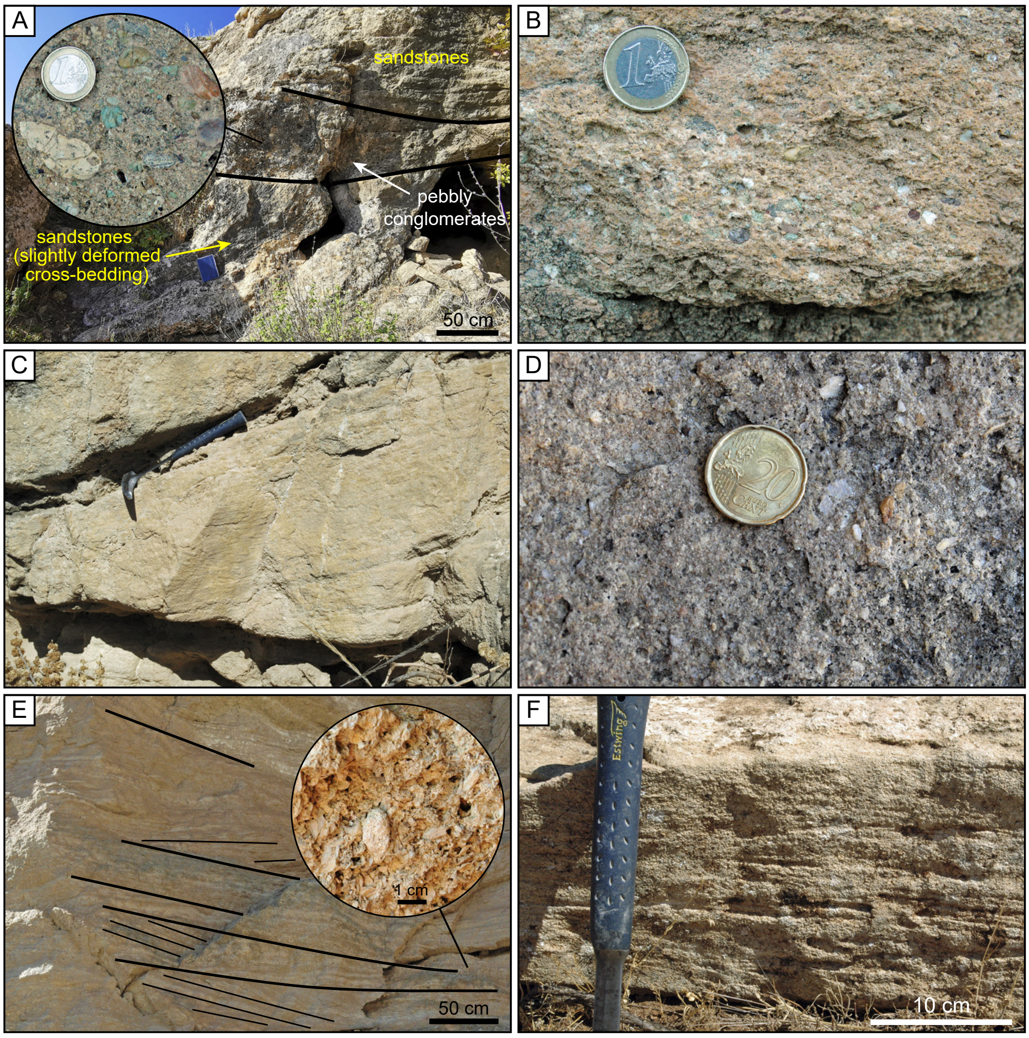
A
sandstones
pebbly conglomerates
sandstones (slightly deformed cross-bedding)
50 cm
B
C
D
E
1 cm
50 cm
F
Estwing
10 cm

Figure 4

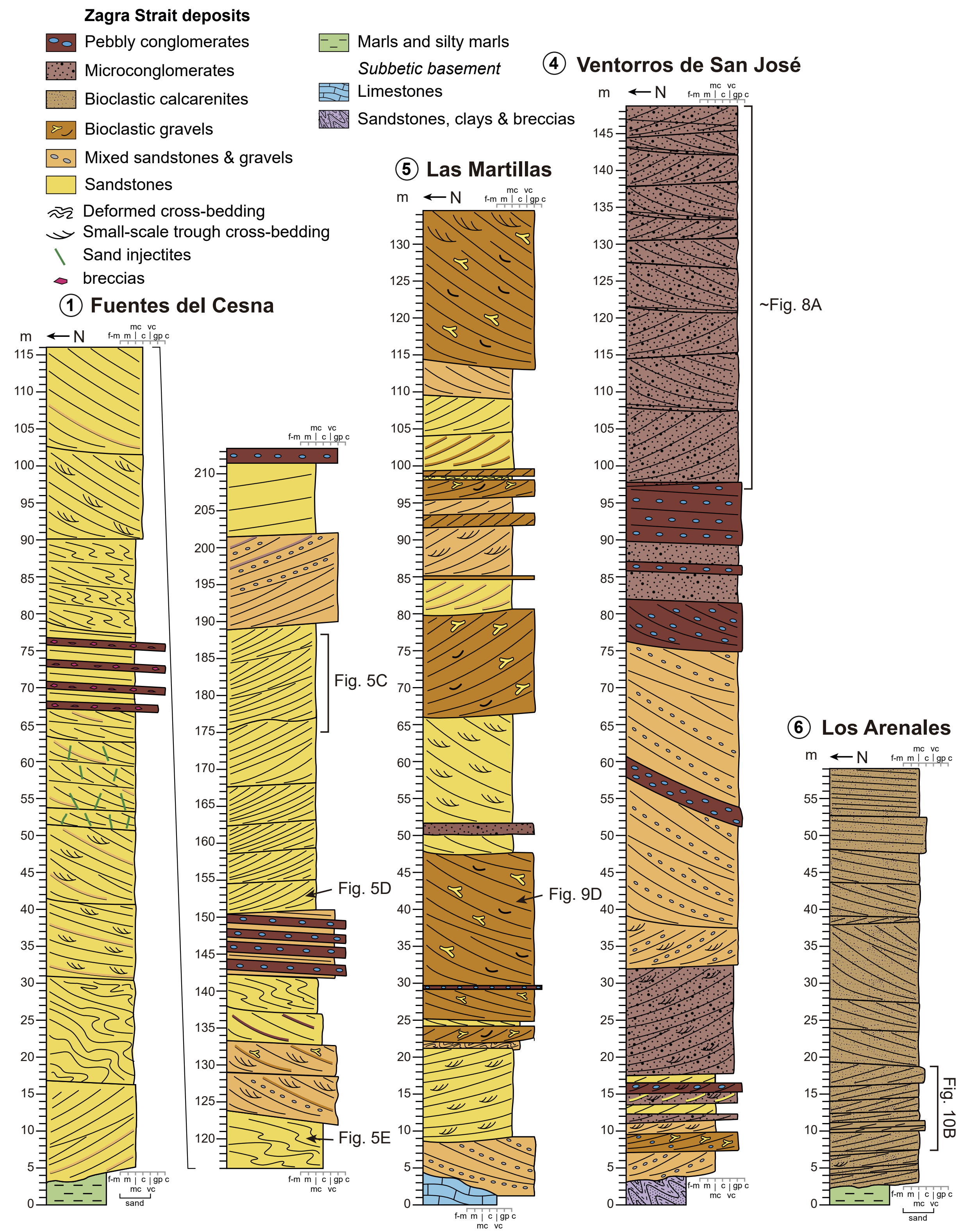

Zagra Strait deposits
Pebbly conglomerates
Microconglomerates
Bioclastic calcarenites
Bioclastic gravels
Mixed sandstones & gravels
Sandstones
Deformed cross-bedding
Small-scale trough cross-bedding
Sand injectites
breccias
Marls and silty marls
Subbetic basement
Limestones
Sandstones, clays & breccias
1 Fuentes del Cesna
5 Las Martillas
4 Ventorros de San José
6 Los Arenales
m
N
f-m m mc c vc gp c
sand
Fig. 5C
Fig. 5D
Fig. 5E
Fig. 9D
~Fig. 8A
Fig. 10B

Figure 5

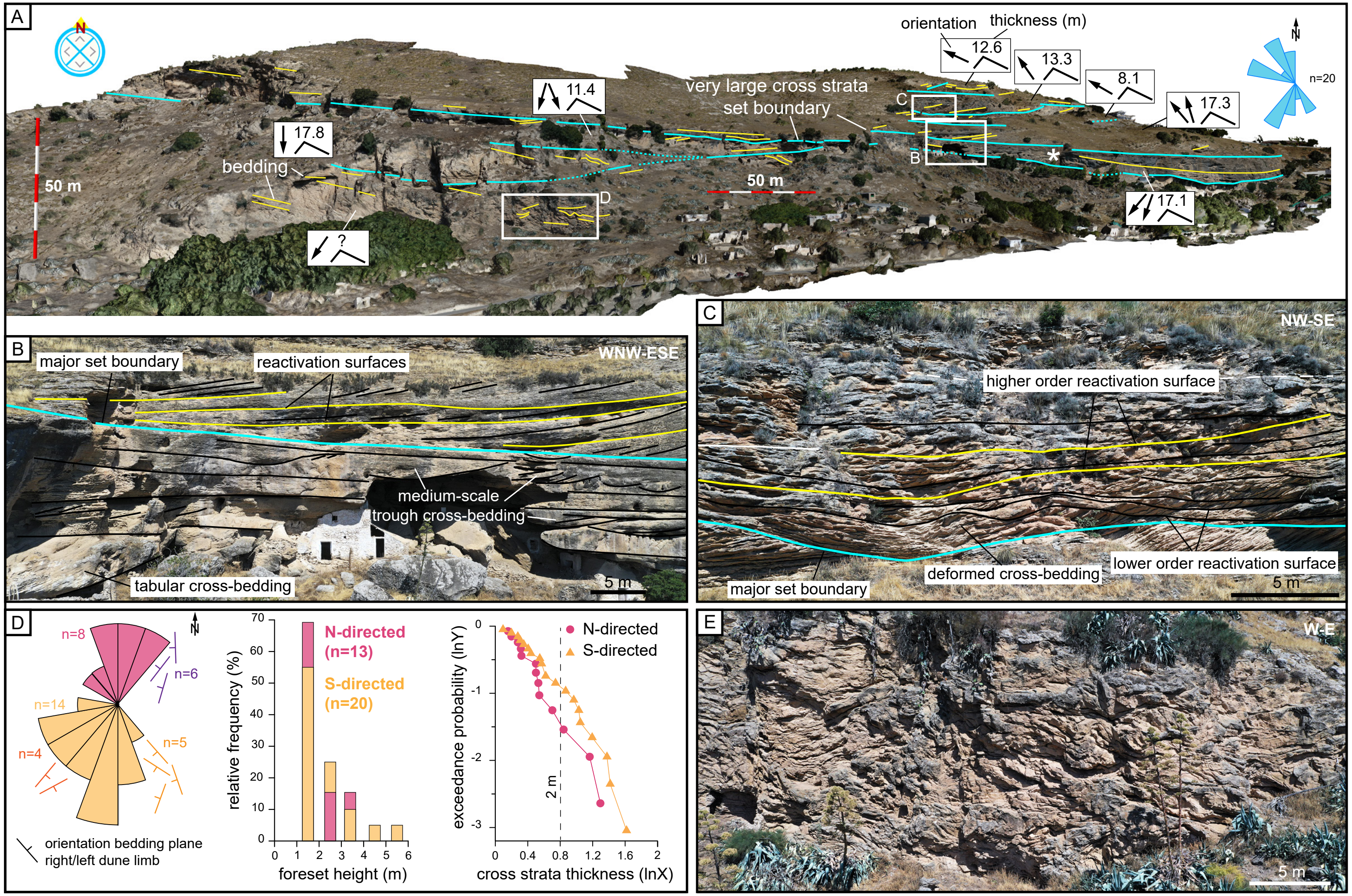

A
orientation
thickness (m)
12.6
13.3
8.1
17.3
17.1
11.4
17.8
?
very large cross strata
set boundary
bedding
50 m
50 m
n=20
B
major set boundary
reactivation surfaces
WNW-ESE
medium-scale
trough cross-bedding
tabular cross-bedding
5 m
C
NW-SE
higher order reactivation surface
lower order reactivation surface
deformed cross-bedding
major set boundary
5 m
D
n=8
n=6
n=14
n=4
n=5
orientation bedding plane
right/left dune limb
N-directed
(n=13)
S-directed
(n=20)
relative frequency (%)
foreset height (m)
exceedance probability (lnY)
cross strata thickness (lnX)
2 m
E
W-E
5 m

Figure 6

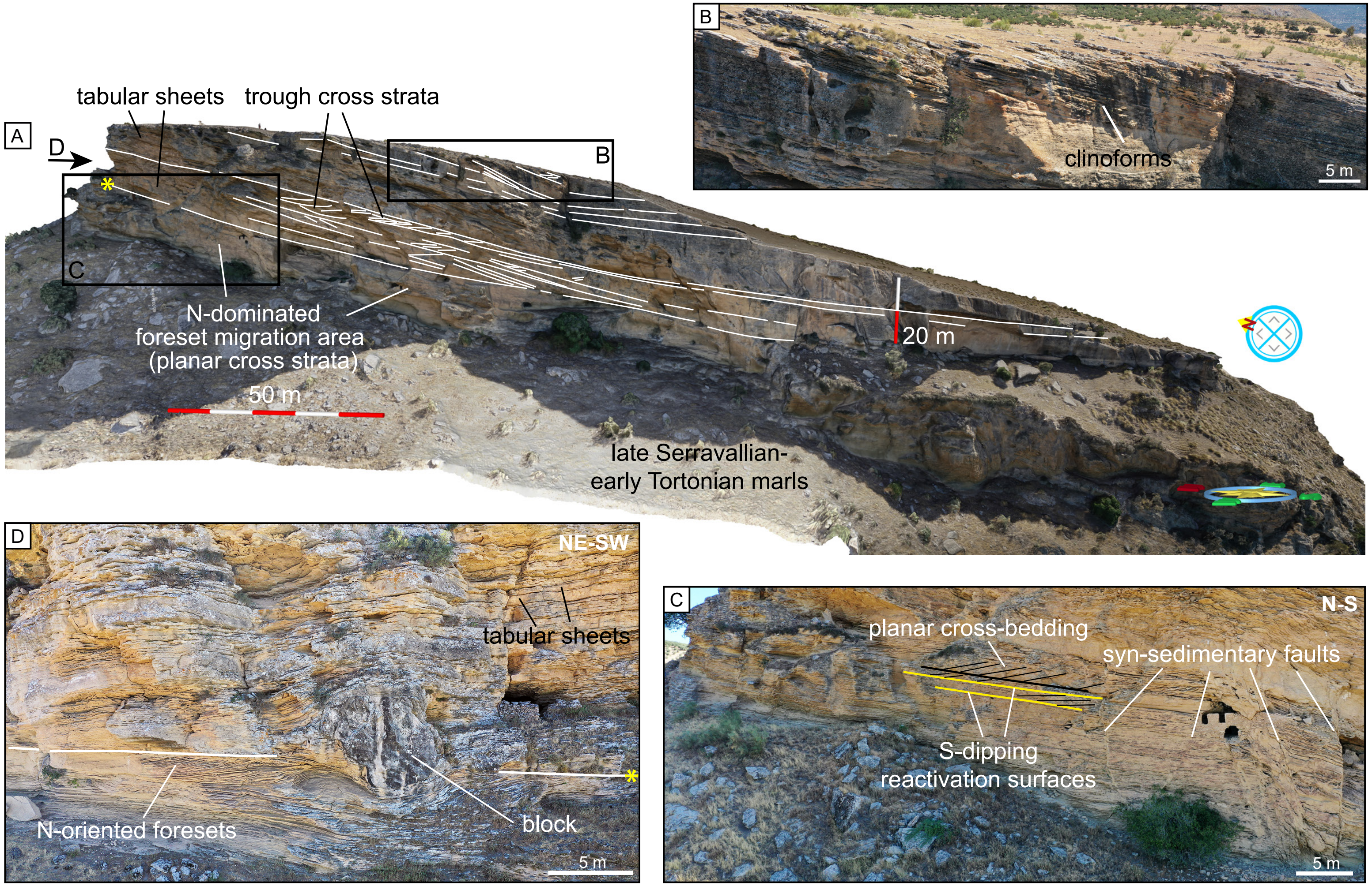
A
tabular sheets
trough cross strata
D
B
C
N-dominated
foreset migration area
(planar cross strata)
50 m
20 m
late Serravallian-
early Tortonian marls
clinoforms
5 m
NE-SW
tabular sheets
N-oriented foresets
block
5 m
N-S
planar cross-bedding
syn-sedimentary faults
S-dipping
reactivation surfaces
5 m

Figure 7

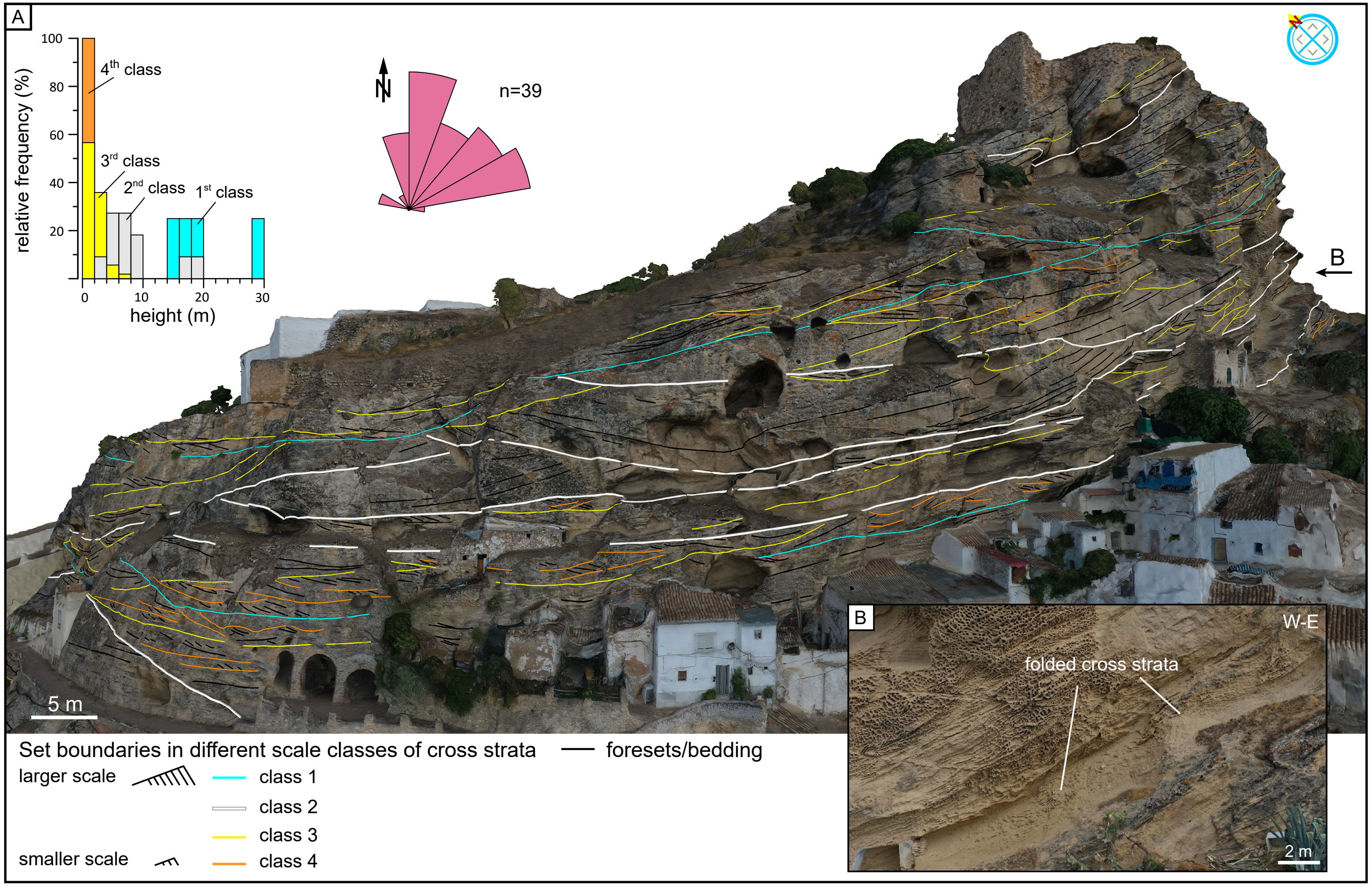
A
relative frequency (%)
100
80
60
40
20
4th class
3rd class
2nd class
1st class
0
10
20
30
height (m)
N
n=39
B
5 m
B
W-E
folded cross strata
2 m
Set boundaries in different scale classes of cross strata
foresets/bedding
larger scale
smaller scale
class 1
class 2
class 3
class 4

Figure 8

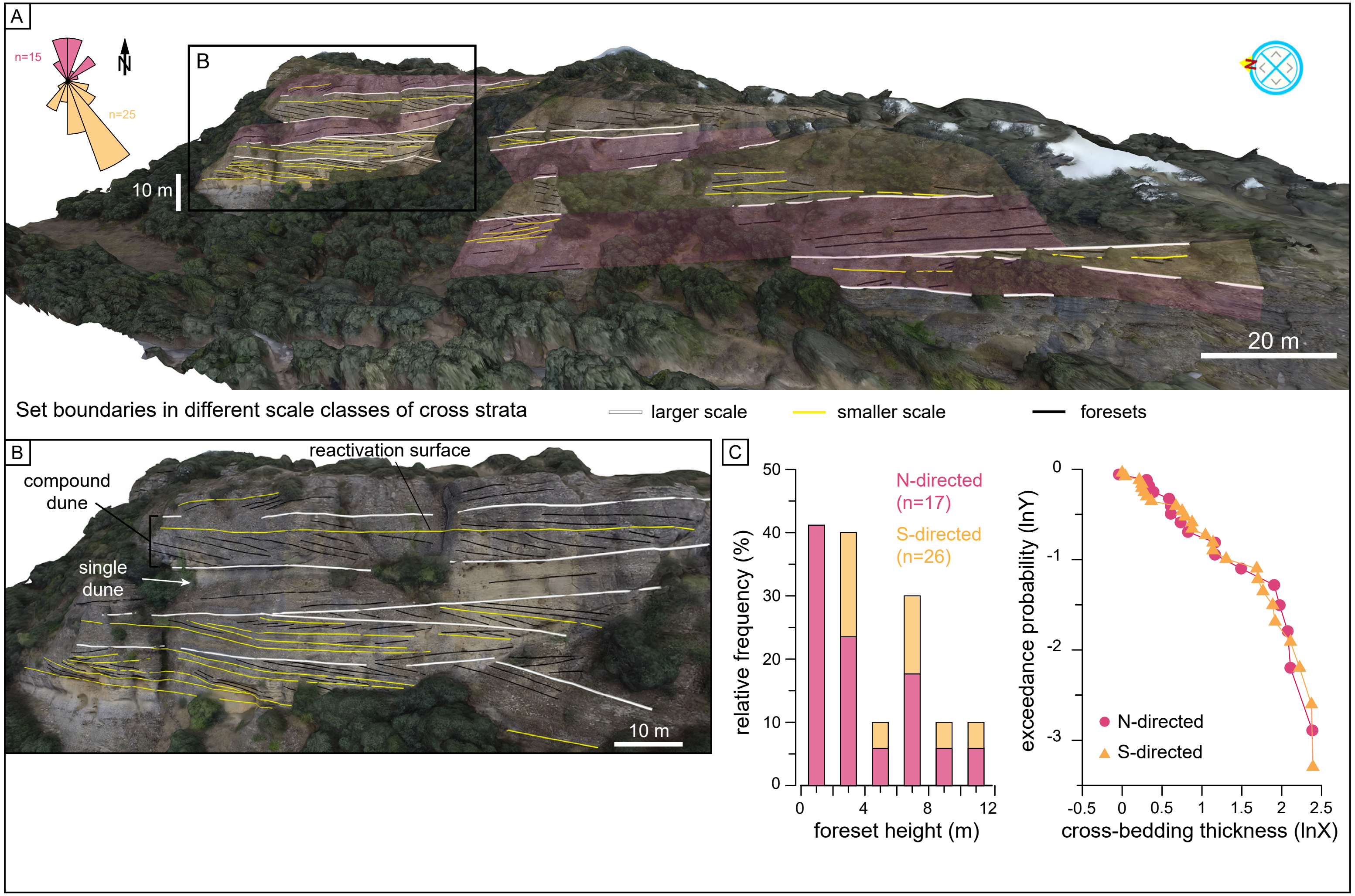
A
n=15
n=25
N
B
10 m
20 m
Set boundaries in different scale classes of cross strata
larger scale
smaller scale
foresets
B
reactivation surface
compound
dune
single
dune
10 m
C
N-directed
(n=17)
S-directed
(n=26)
relative frequency (%)
foreset height (m)
exceedance probability (lnY)
cross-bedding thickness (lnX)
N-directed
S-directed

Figure 9

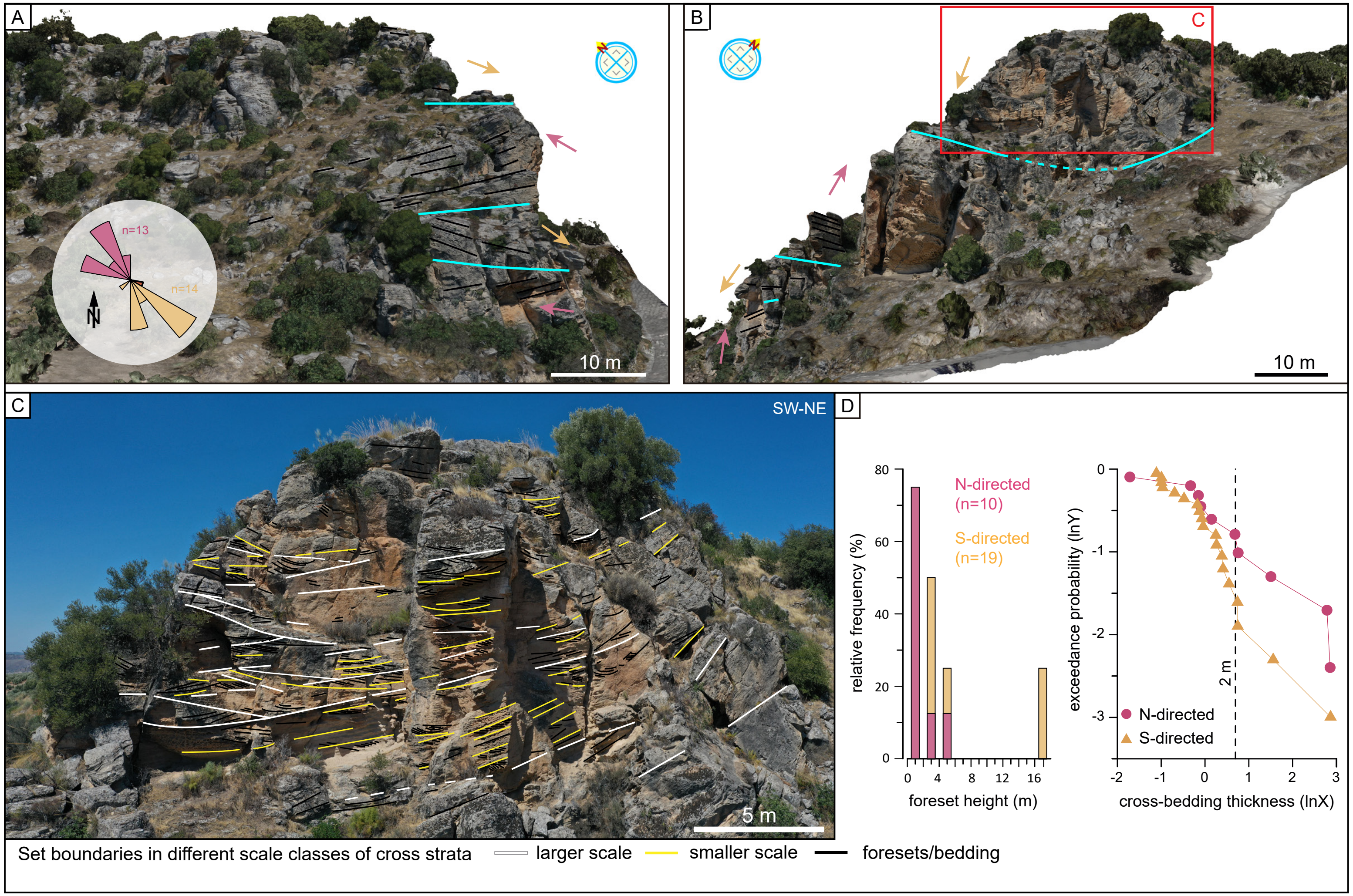

A
n=13
n=14
N
10 m
B
C
10 m
C
SW-NE
5 m
D
relative frequency (%)
foreset height (m)
N-directed (n=10)
S-directed (n=19)
exceedance probability (lnY)
cross-bedding thickness (lnX)
2 m
N-directed
S-directed
Set boundaries in different scale classes of cross strata
larger scale
smaller scale
foresets/bedding

Figure 10

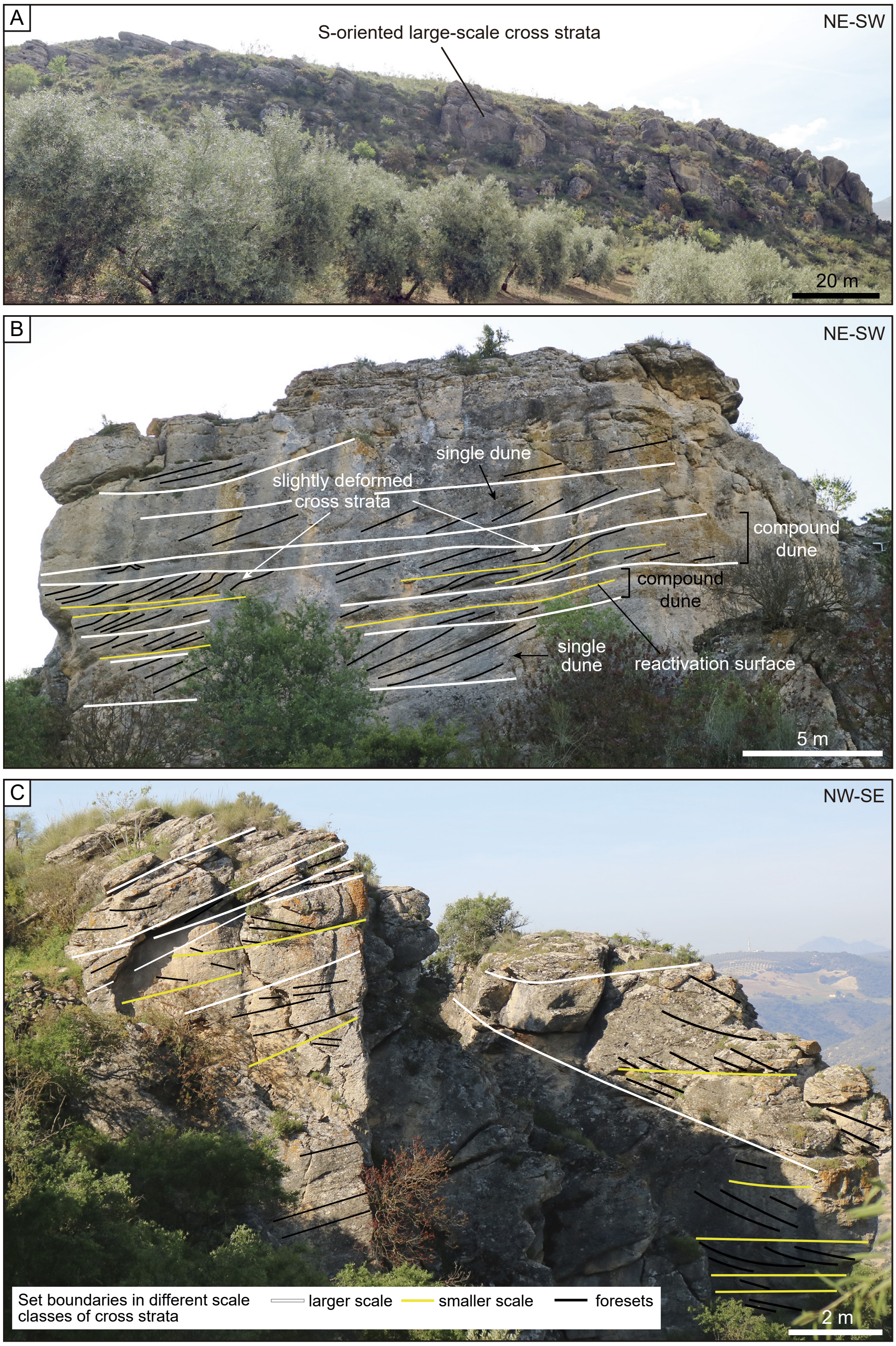
A
S-oriented large-scale cross strata
NE-SW
20 m
B
NE-SW
single dune
slightly deformed
cross strata
compound
dune
compound
dune
single
dune
reactivation surface
5 m
C
NW-SE
Set boundaries in different scale
classes of cross strata
larger scale
smaller scale
foresets
2 m

Figure 11

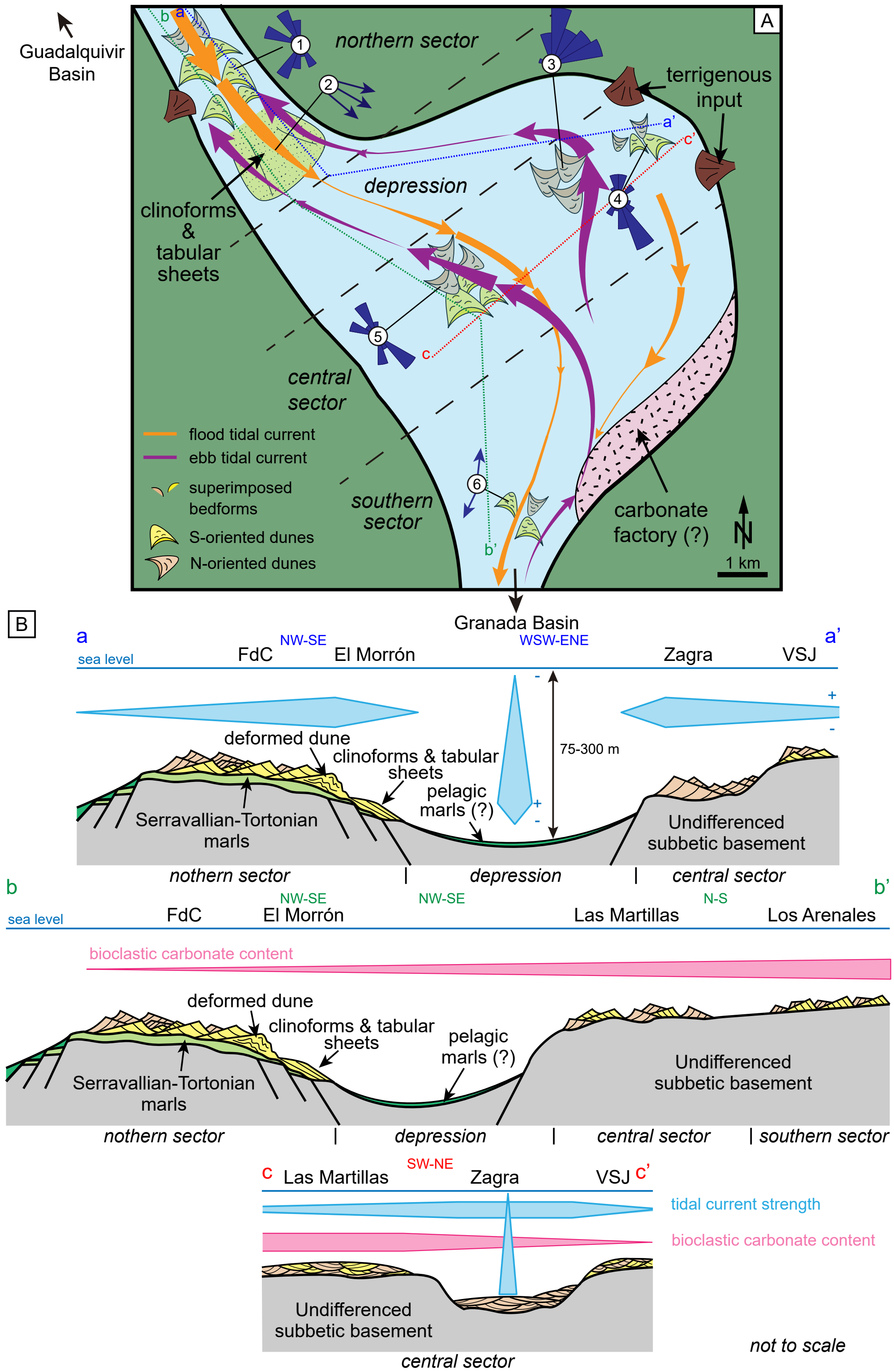
A
Guadalquivir Basin
northern sector
terrigenous input
clinoforms & tabular sheets
depression
central sector
southern sector
carbonate factory (?)
flood tidal current
ebb tidal current
superimposed bedforms
S-oriented dunes
N-oriented dunes
1 km
Granada Basin
B
a
a'
sea level
NW-SE
WSW-ENE
FdC
El Morrón
Zagra
VSJ
deformed dune
clinoforms & tabular sheets
pelagic marls (?)
75-300 m
Serravallian-Tortonian marls
Undifferenced subbetic basement
nothern sector
depression
central sector
b
b'
NW-SE
N-S
Las Martillas
Los Arenales
bioclastic carbonate content
southern sector
c
c'
SW-NE
tidal current strength
not to scale

Figure 12

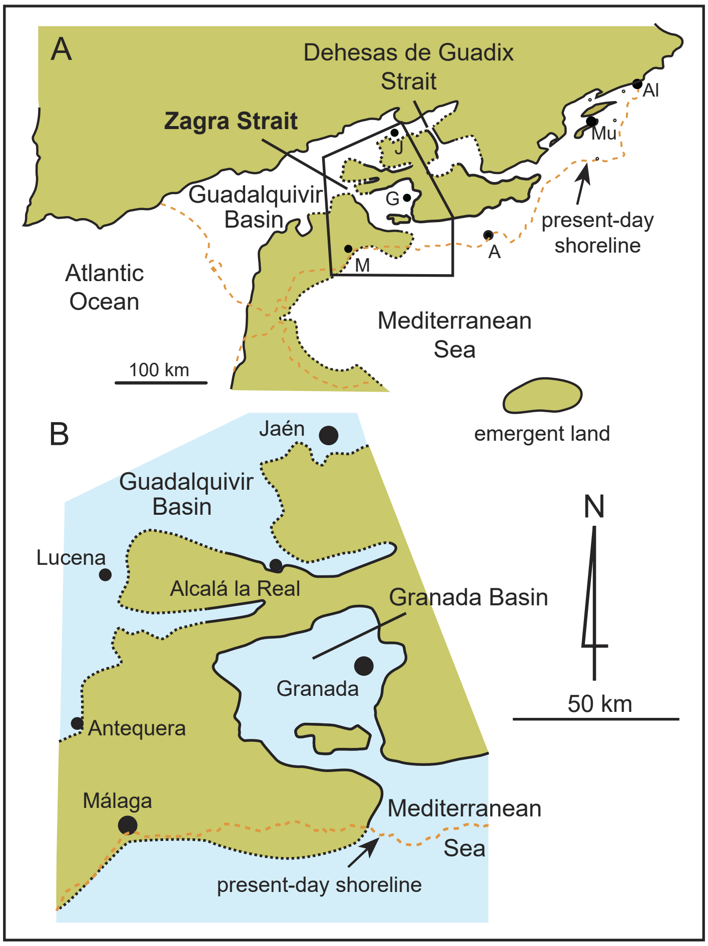
A
Dehesas de Guadix
Strait
Zagra Strait
J
Al
Mu
G
Guadalquivir
Basin
present-day
shoreline
A
M
Atlantic
Ocean
Mediterranean
Sea
100 km
emergent land
B
Jaén
Guadalquivir
Basin
N
Lucena
Alcalá la Real
Granada Basin
Granada
50 km
Antequera
Málaga
Mediterranean
Sea
present-day shoreline